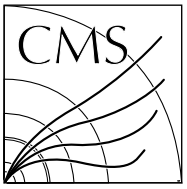

The Compact Muon Solenoid Experiment

CMS Note

Mailing address: CMS CERN, CH-1211 GENEVA 23, Switzerland

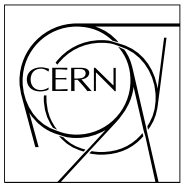

May 12, 2006

Prospects for the precision measurement of the W mass with the CMS detector at the LHC.

V. Büge, Ch. Jung,

Inst. f. Experimentelle Kernphysik, Universität Karlsruhe, 76128 Karlsruhe, Germany
and Institut für Wissenschaftliches Rechnen, Forschungszentrum Karlsruhe, 76344 Eggenstein-Leopoldshafen, Germany

G. Quast,

Inst. f. Experimentelle Kernphysik, Universität Karlsruhe, 76128 Karlsruhe, Germany

A. Ghezzi, M. Malberti, T. Tabarelli de Fatis

Università di Milano-Bicocca and INFN, Piazza della Scienza 3, I-20126, Milano, Italy

Abstract

The precise measurement of the mass of the W boson constitutes an important consistency check of the Standard Model and, together with the top quark mass, is sensitive to supersymmetric corrections. In this note, methods are presented which employ the large number of Z bosons produced at the LHC to significantly reduce theoretical and experimental uncertainties on the W mass measurement. A precision of about 40 MeV (20 MeV) with the first 1 fb^{-1} (10 fb^{-1}) of integrated luminosity during the low luminosity run of the LHC is expected.

1 Introduction

An improved measurement of the W mass at the LHC, combined with other electroweak measurements (i.e. m_{top} and $\sin^2_{\theta_W}$), will lead to fix strong indirect constraints on M_H, the mass of the Standard Model Higgs boson. After the discovery of the Higgs boson at the LHC, high precision measurements of the W boson and the top quark masses will allow a stringent consistency check of the Standard Model. To ensure that the experimental errors on m_{top} and M_W equally contribute to the uncertainty on M_H (the other electroweak parameters being far better measured), the precision on m_{top} and M_W has to satisfy the following relation [1]:

$$\Delta M_W \sim 0.7 \times 10^{-2} \Delta m_{top}$$

The mass of the top quark is foreseen to be measured at the LHC with an accuracy better than 2 GeV [2]. It follows that a global precision on M_W of about 15 MeV has to be achieved, to avoid it to be the dominant error in the estimate of M_H. Such a precision measurement of the W mass at the LHC becomes feasible because a huge sample of data available at the LHC will guarantee a small statistical error and a good control of the systematic effects.

At hadron colliders, the W mass measurement is performed through the study of the leptonic decays $W \to \mathrm{l}\nu$ ($\mathrm{l} = \mathrm{e}, \mu$) with the comparison between the experimental distribution of the W transverse mass and Monte Carlo templates generated at different values of M_W. At the LHC the total cross section $\sigma\,(pp \to W^{\pm}) \cdot BR(W \to \mathrm{e}\nu$ or $\mu\nu)$ for the production of W bosons decaying into one lepton and the corresponding neutrino is about 30 nb. Then about 300 millions of events are expected with 10 fb^{-1}of integrated luminosity. This large sample of data will ensure a nearly negligible statistical error ($\sim$2 MeV [1]). The most relevant contributions to the systematic uncertainties on the measurement of the W mass come from the lepton energy/momentum scale, the lepton energy/momentum resolution, the modelling of the system recoiling against the W boson, the parton distribution functions, the W intrinsic width, the radiative decays and the background. All these contributions should be kept below about 10 MeV to achieve the aimed precision of 15 MeV on M_W, combining channels and experiments. To accomplish this, new strategies for the W mass measurements must be considered. The most promising one consists in predicting the distribution of experimental observables sensitive to the W mass, such as the transverse momentum or energy of the charged lepton (p_l^T) and/or the transverse mass of the boson (m_T), from the corresponding distribution measured in Z boson decays into two charged leptons. The transverse mass of the W boson is defined by

$$m_T = \sqrt{2 p_l^T p_\nu^T (1 - \cos(p_l^T, p_\nu^T))} \tag{1}$$

where p_l^T, p_ν^T and $\cos(p_l^T, p_\nu^T)$ are the transverse momenta of the charged lepton, of the neutrino and the cosine of their angle, respectively. The concept of transverse mass measurement, and in general the selection of Z events to mimic W events, can be applied to Z boson events regarding one of the reconstructed leptons as missing energy. The theoretical description of both decays is similar and the resulting distributions in transverse mass are comparable for a wide range in kinematics.

The advantage of this approach is that most of the experimental and theoretical uncertainties, being common between W and Z, cancel in the comparison, leading to a global reduction of the systematic uncertainty. The drawback is a larger statistical uncertainty due to the smaller production rate of Z bosons decaying to charged leptons, being the cross section for the process $pp \to Z$ with $Z \to \mathrm{e}^+\mathrm{e}^-$ or $\mu^+\mu^-$ about 1/10 of the corresponding W cross section. A statistical precision of order 10 (40) MeV for an integrated luminosity of 10 (1) fb^{-1} is anticipated. Besides any statistical consideration, the full exploitation of this approach requires a detailed understanding of the experimental apparatus, of its calibration and resolution and might be difficult at the early stages of the experiment. Still, just because most of the instrumental effects are cancelled by this approach, it seems to provide the best way to get an early measurement of the W mass from the first 1 fb^{-1} of data.

In this paper, after a conceptual description of the analysis methods, with details on their theoretical motivation (Section 2), a description of the experiment simulation and of the data samples is given (Section 3). Section 4 and 5 describe the analyses of $W \to e\nu$ and $W \to \mu\nu$ decays respectively, with discussion of the signal selection and backgrounds and a detailed account of the statistical and systematical uncertainties expected for the first 1 fb^{-1} and the final 10 fb^{-1} of data integrated in the low luminosity phase of the LHC ($\mathcal{L} = 10^{33}$ cm^{-2}s^{-1}).

In the analysis of $W \to e\nu$ events, we assume a detector configuration with a fully operational electromagnetic calorimeter both in the barrel and in the end-caps. The analysis is mainly based on the calorimetric measurement of the electron energy and is only mildly dependent on the performance of the tracking devices for the electron identification, the measurement of its direction and some isolation criteria.

In the analysis of $W \to \mu\nu$ events, the use of missing energy requires a fully functional calorimeter, and the muon momentum measurements requires a fully functional tracker with a well modelled resolution.

2 Analysis strategy

Two different ways to scale Z- to W-boson events are considered in this work. The first one, conceptually discussed in [4], is based on the comparison of the same experimental observables in W- and Z-events scaled to the boson masses. The sensitivity of this method, which can take advantage of the precision calculation of the theoretical ratio of the W- and Z-boson differential production cross-sections, is fully addressed in the analysis of transverse energy distribution of the electrons from $W \to e\nu$ decays. An alternative approach is considered in the analysis of $W \to \mu\nu$ events. It consists predicting W-boson distributions from Z-events by means of Lorentz transformations parameterised as a function of the boson masses and widths. This more phenomenological approach is exploited in the analysis of the transverse mass distributions of Z and W bosons, which are less sensitive to radiative corrections.

2.1 The "Scaled Observable Method"

This analysis strategy is based on the prediction of the experimental distribution for W-boson observables scaled to the boson mass from the corresponding distribution measured for Z-bosons decaying into two charged leptons, along with the theoretical ratio between the W and Z cross-sections, calculated at a fixed perturbative order. Ideally, the differential cross section for the *W* boson as a function of a given observable O^V ($V = W, Z$) can be predicted from the one measured for *Z* boson as:

$$\left.\frac{d\sigma^W}{dO^W}\right|_{pred} = \frac{M_Z}{M_W} R(X) \left.\frac{d\sigma^Z}{dO^Z}\left(O^Z = \frac{M_Z}{M_W} O^W\right)\right|_{meas}, \tag{2}$$

where $R(X) = \frac{d\sigma^W}{dX^W} / \frac{d\sigma^Z}{dX^Z}$ is the ratio, deduced from theoretical calculations, between the differential cross sections in terms of the scaled variable $X^V = \frac{O^V}{M^V}$. The parameter M_W can be extracted by comparing this prediction to the distribution for W events observed in the experiment. In practice, additional corrections to $R(X)$ are needed to account for the acceptance to Z and W events and for the experimental resolution. This calls for a detailed understanding of the detector response by means of Monte Carlo simulations compared to control samples. Clearly, the definition of $R(X)$ is the most critical aspect and must include both detector effects and theoretical predictions. This will be further addressed along with the discussion of the systematic limitations.

The precise knowledge of the Z boson mass (about 2 MeV) implies no intrinsic limitations to the accuracy of this approach. Moreover, it has been demonstrated [4] that the ratio between W- and Z-boson observables can be reliably calculated using perturbative QCD, even when the individual W- and Z-boson observables are not. This analysis strategy is particularly relevant to the measurement of the W mass through the measurement of the lepton transverse momentum distribution, otherwise limited by the large radiative corrections affecting the prediction of the $p^T(W)$ spectrum. Because of this, the measurement of the W mass has been traditionally addressed through the analysis of the boson transverse mass distribution, which is less sensitive to radiative corrections, but depends on the neutrino transverse momentum reconstruction and is plagued by larger experimental uncertainties. The complementarity between these two observables is well represented in Fig. 1, which shows the distribution of m_T and E^T as expected in CMS for $W \to e\nu$ decays and compared to the case of perfect detector resolution and of zero p^T of the W boson. The reconstruction of the transverse mass is dominantly affected by the experimental resolution on the missing transverse energy (neutrino transverse momentum), which is also dependent on the machine parameters, through pile-up events. On the other hand, the E^T spectrum of the lepton is mainly affected by the p_T distribution of the W boson production, while the additional effect of the resolution on the lepton p_T, which in case of electrons is best estimated from the energy deposited in the calorimeter, is marginal at all the luminosities.

The outlined approach makes the analysis of the lepton E^T or p^T attractive, as a reliable prediction of its distribution in W-boson events is in principle possible. In the following we will specialise the analysis to this observable for the $W \to e\nu$ decays. Given the aimed precision at LHC, a calculation of the W- to Z-boson differential cross-section ratio as a function of the scaled lepton transverse energy with a precision of order 1% or better is required. The ratio of the available calculations at the NLO to the LO in α_S shows that the perturbative series is well behaved. The contribution from the missing orders has been verified to be at the 1% level, by studying the dependence of the NLO prediction on the renormalisation and factorisation scales. A more careful analysis of these aspects is required to evaluate the ultimate precision achievable with this method. Noteworthily, should the precision turn out to be insufficient, the extension of the calculation one order higher in α_S is technically feasible [4].

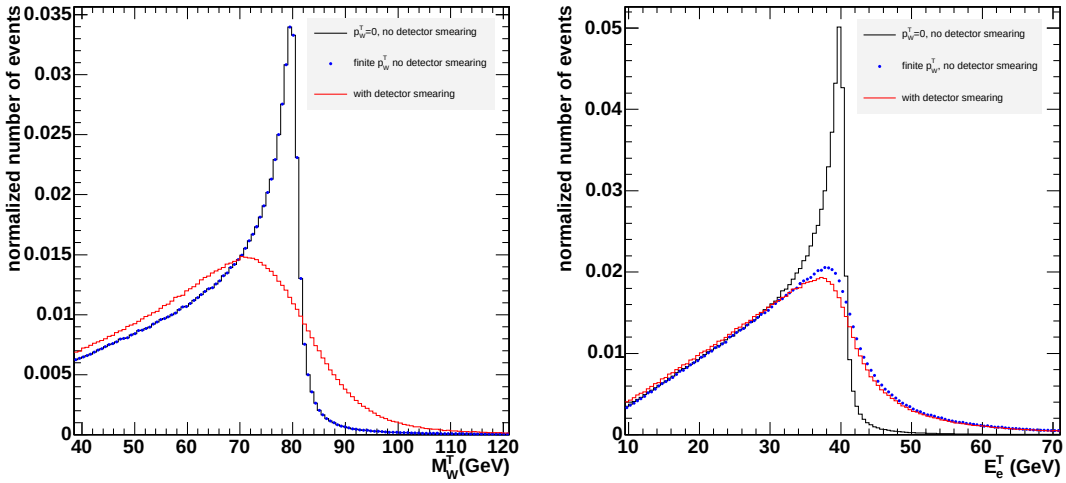

Figure 1: Boson transverse mass (left) and electron transverse momentum (right) distributions in $W \to e\nu$ decays. The distributions at the generator level with $p^T(W) = 0$ (black line), with finite W boson p^T (dots) and including the experimental resolution in the low luminosity phase are shown (red line).

On the other hand, large cancellations occurs for the differential cross-section ratio of the scaled transverse mass distributions and calculations seems already sufficiently precise. On the experimental side, an analysis based on the transverse mass is definitely more challenging and also less transparent, as the limited experimental resolution on the transverse mass implies larger corrections to the weighting function $R(X)$. A careful study of the systematic limitations of instrumental origin entering the analysis of the scaled transverse mass distribution is not finalised yet and the study of this observable will not be discussed in detail for $W \to e\nu$ events. This observable is considered in the analysis of $W \to \mu\nu$ events in the next section.

2.2 The "Morphing Method"

Similarly to the previous method, this approach exploits the similarity between the theoretical descriptions of W- and Z-boson production and decay processes. The idea is to transform measured Z boson events into W boson events, called *morphed events*. After correcting for unavoidable differences by appropriate re-weighting of the distributions, the resulting transverse mass distribution can then be compared with the measured W data. The proposed transformation procedure [5] is straight-forward:

1. Starting with an event containing a Z boson candidate, the two muons are used to reconstruct the Z. Then, both muons are boosted to the rest frame of the boson.

2. The mass of the Z boson M_Z^{in} is reduced to a value M_Z^{out} according to the mass difference between M_Z and the assumed mass M_Z^{morph} of the W boson. Taking account of the different widths of the underlying Breit-Wigner distributions of W and Z bosons, Γ_W and Γ_Z, respectively, results in

$$M_Z^{out} = (M_Z - M_Z^{in})\frac{\Gamma_W}{\Gamma_Z} + M_Z^{morph}\,, \tag{3}$$

   where M_Z is the true mass of the Z in the event, and $\Gamma_W = 2.124$ GeV [6].

3. The momenta of the final states have to be changed according to the new mass M_Z^{out} of the boson. They are recalculated assuming a two body decay of the mass-reduced boson into a muon and a neutrino. The directions of the final states, back-to-back in the boson's rest frame, remain unchanged in this process.

4. The system is boosted back to the detector frame assuming that the boson acquires the same momentum as before the transformation.

5. Known differences in production and decay of Z and W bosons are remedied by re-weighting of the modified Z events in a last step.

The event obtained in this way is comparable with an event containing the decay of a W boson with mass M_Z^{out}. The transformation is repeated for different values in mass, and the resulting distributions of the transverse mass are compared with the distribution measured for W boson candidates. While ensuring conservation of momentum by construction, the proposed method does not conserve four-momentum, as the system recoiling against the boson is not adapted to the new mass.

As an illustration of the method, the resulting distributions for three different values of M_Z^{morph} are presented in Fig. 2 together with the distribution of real W events. Detector effects are taken into account only by smearing the muon momenta of the generated events according to the expected detector resolution. Cuts as well as effects arising from the resolution of the missing transverse energy are not applied yet.

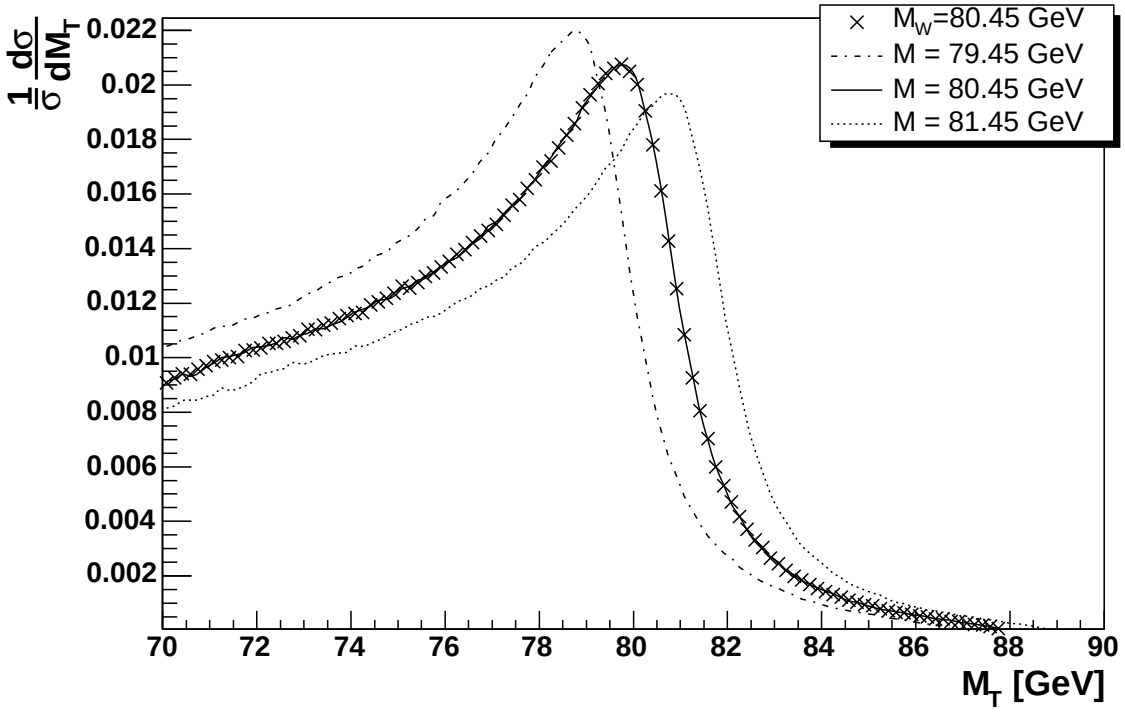

Figure 2: Transformed transverse mass distributions for three different masses. The solid line represents the transformation of a Z boson event to the mass of the generated W boson, M_W. The two curves drawn with dotted and dot-dashed lines represent transformations to a mass $M_Z^{morph} = M_W \pm$ 1GeV. The distribution of the transverse mass of the W boson is shown with crosses.

The main advantage of this method is that it is only sensitive to differences between W and Z boson production and decay properties. Influences from detector uncertainties or miscalibrations should largely cancel out, as long as they affect both processes in the same way.

This method has been studied in detail with $Z \to \mu\mu$ and $W \to \mu\nu$ decays, and the effects of various systematic uncertainties are evaluated.

3 Simulation details

In order to be not limited by statistics, the analyses are performed using large data samples produced with FAMOS for a fast simulation of the CMS detector [9].
$W \to e\nu$ events were generated with PHYTIA 6.227 [7] using the CMS software package CMKIN [8] to interface the generator to the detector simulation. The reliability of the fast simulation of the detector response has been evaluated by comparisons to data samples produced through the full simulation and reconstruction chain of the CMS experiment (ORCA) [9]. In the signal definition, the single W production process was considered. The description of this process in the PYTHIA 6.227 generator, at the first order in α_S, though inadequate for the final experiment, is sufficient to address the statistical and systematical uncertainties of instrumental origin. Theory uncertainties are separately discussed in Section 4.2.

For the $W \to e\nu$ analysis, the fast simulated samples are the following ones:

- 27×10^6 $W \to e\nu$ events, with M_W = 80.45 GeV;
- 12.5×10^6 $Z/\gamma^* \to e^+e^-$ events, with M_Z = 91.187 GeV and M_{ee} >50 GeV;

Smaller samples of fully simulated events are used for cross checks. About 200 000 events belonging to a fully simulated $W \to e\nu$ dataset have been studied for such purpose. This dataset was generated with preselection cuts (p_e^T >25 GeV and $|\eta|$ <2.7) and the digitisation was performed within the ORCA framework including the effects of pile-up at low luminosity (2×10^{33} cm^{-2}s^{-1}).

Also for the W$\to$ $\mu\nu$ channel large datasets were generated with PYTHIA 6.320 using CMKIN and then were passed through the fast simulation of CMS including low luminosity pile-up. The total sample of events consists of

- 21×10^6 $W \to \mu\nu$ events with M_W=80.45 GeV;
- 11×10^6 $Z \to \mu\mu$ events with M_Z=91.188 GeV.

A full detector simulation of $W \to \mu\nu$ events was available from an unbiased sample which contains about 200 000 events digitised with ORCA and includes pile-up at low luminosity.

Electron definition An electron is characterised by a supercluster in the electromagnetic calorimeter and a track pointing towards it. Compatibility between the supercluster and track angular position and energy estimate are required to select electrons among electron candidates in an event [9]. Moreover, the energy deposition in the calorimeters is required to be consistent to the one expected from an electron. An isolation criterion is also applied, as electrons from W and Z decays are expected to be well isolated from possible hadron jets in the event. This is accomplished through the following set of selections:

- The difference in pseudo-rapidity between the track and the supercluster in the electromagnetic calorimeter is required to satisfy $\Delta\eta = |\eta_{trk} - \eta_{clus}| < 0.005$;
- The variable $|1/E - 1/P|$, where E is the energy of the supercluster and P the momentum of the matching track is required to be lower than 0.02;
- The ratio between the energy deposited in the electromagnetic calorimeter and the energy deposited in the hadron calorimeter is required to be lower than 0.05;
- The ratio between the energy of the supercluster and the momentum of the associated track is required to exceed 0.8;
- the track isolation, defined as the sum over all the tracks (except the electron track) in a cone of radius $R = \sqrt{(\Delta\eta)^2 + (\Delta\phi)^2}$ around the supercluster direction, divided by the transverse energy of the supercluster:

$$Iso = \frac{1}{E_{SC}^T}\left(\sum_{r<R} p_{track}^T - p_e^T\right) \tag{4}$$

  is required to be lower than 0.2.

The electron transverse energy spectra in $W \rightarrow e\nu$ events obtained from FAMOS and ORCA simulations after their criteria are in good agreement, as shown in Fig. 3. The RMS of the $(E^T_{e,reco} - E^T_{e,true})$ distribution is about 1.4 GeV both in ORCA and FAMOS samples. The mean of the distribution is also consistent in the two simulation programs.

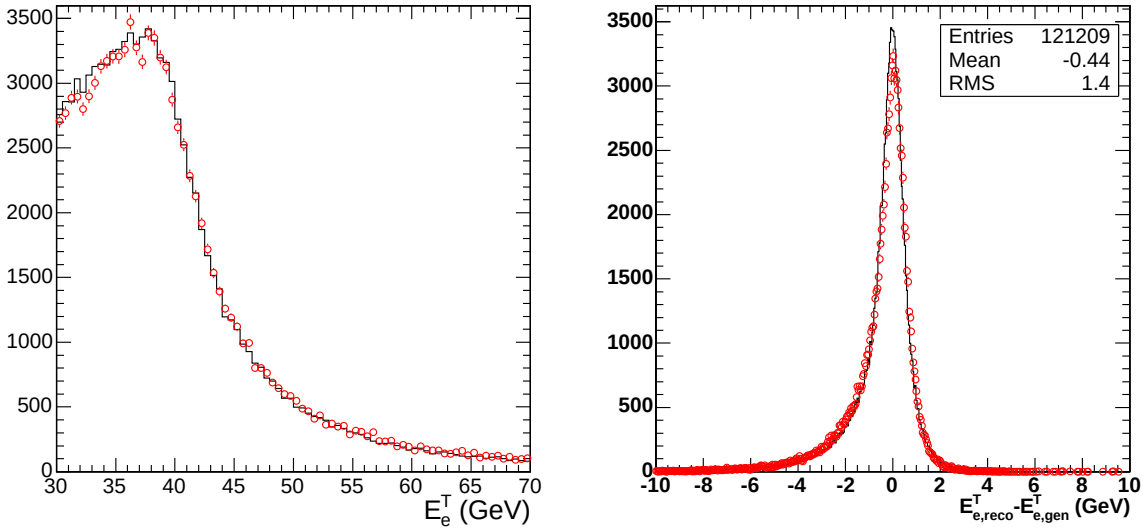

Figure 3: The transverse energy spectrum of the electron in $W \rightarrow e\nu$ events (left) and the resolution (right). The distributions obtained with FAMOS (solid line) and ORCA (open dots) are shown.

Muon definition For the reconstruction of the muons, the Global Muon Reconstructor is used. This method and its properties are described in detail in Volume I of the CMS Physics TDR [9].

In Fig. 4, the relative resolution of the transverse momentum of the muon is shown. The comparison of the full with the fast detector simulation shows that both simulations tend to larger reconstructed p^T compared to generator information. The magnitude of these differences is at the scale of one-tenth of a percent. It is obvious that both distributions are not symmetric. In addition, the relative resolution of p^T differs between the FAMOS and the OSCAR simulation. For the latter, the mean of the distribution is $(3.56 \pm 0.14) \cdot 10^{-3}$. On average the reconstructed transverse momentum of the muons according to the fast simulation is too large by a factor of $(2.61 \pm 0.02) \cdot 10^{-3}$.

In addition, the shift to larger values of the reconstructed P_T of the muon depends on the absolute value of the transverse momentum itself. The study with FAMOS has shown that the observed shift increases from $1.92 \pm 0.04 \cdot 10^{-3}$ for values of p^T between 20 GeV and 30 GeV to $4.50 \pm 0.05 \cdot 10^{-3}$ for higher values of the transverse momentum between 40 GeV and 50 GeV.

The resolution of the angular variables, θ and ϕ, has also been studied with both ORCA and FAMOS. The distributions are symmetric and the mean values compatible with zero. FAMOS, however, predicts slightly wider distributions than ORCA. The differences between Oscar and the real detector in 2007 will need to be understood better than the present differences between FAMOS and OSCAR for precision measurements. A valuable monitoring quantity is the distribution of the Z boson mass as determined from the reconstructed muons. Its mean value allows for calibration of the average momentum scale of the muons, and the width provides information on the angular and momentum resolution. A comparison of the simulations of the reconstructed Z mass with FAMOS and OSCAR/ORCA is shown in Fig. 5 for illustration. The differences discussed above lead to a clearly observable and statistically very significant shift between the mass distributions of the Z boson, amounting to 0.16 GeV. In the real experiment, with an expected number of approximately 500 000 accepted events for an integrated luminosity of 1 fb^{-1}, a comparison of the reconstructed Z mass in real data with the Monte Carlo simulation will detect the presence of such shifts with a very good statistical precision of about ± 5 MeV. Thus, the shape of the reconstructed Z peak will provide an essential monitoring tool to verify the quality of the detector description in the Monte Carlo, and can also be used to tune the simulation.

The Missing Transverse Energy and the neutrino definition The missing transverse energy (MET) gives an estimate of the transverse momentum of the neutrino. It is calculated by taking the sum of the transverse energies of

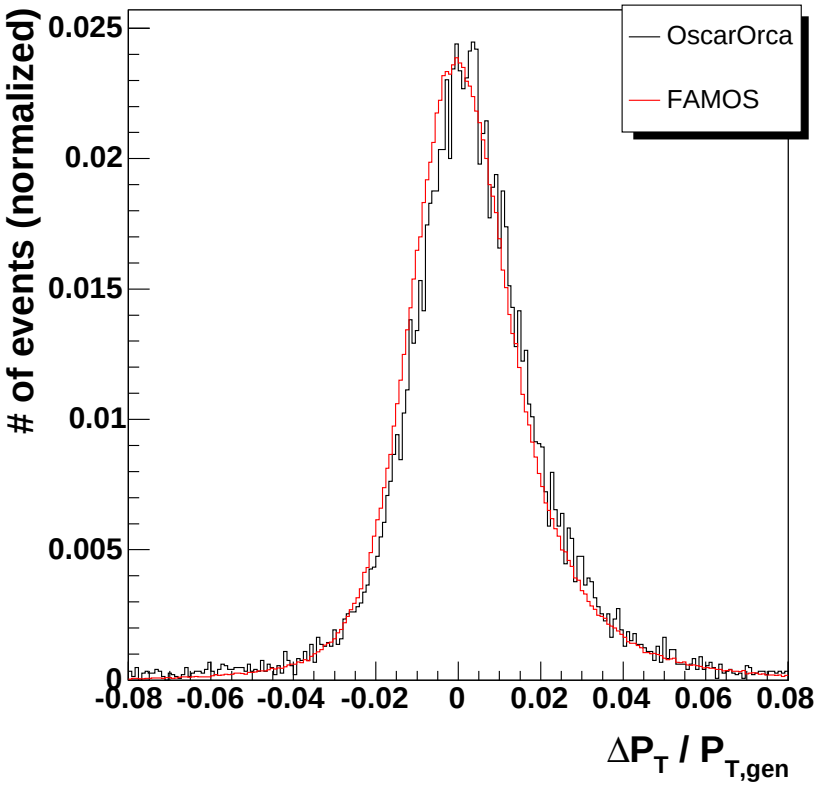

Figure 4: The relative resolution of the transverse momentum from FAMOS is shown in red. Its mean is at $2.6{\cdot}10^{-3}$ with an RMS of $17.4{\cdot}10^{-3}$. The black curve with a mean of $3.5{\cdot}10^{-3}$ and an RMS of $18.7{\cdot}10^{-3}$ shows the results of the full simulation. The bin width is $8{\cdot}10^{-4}$.

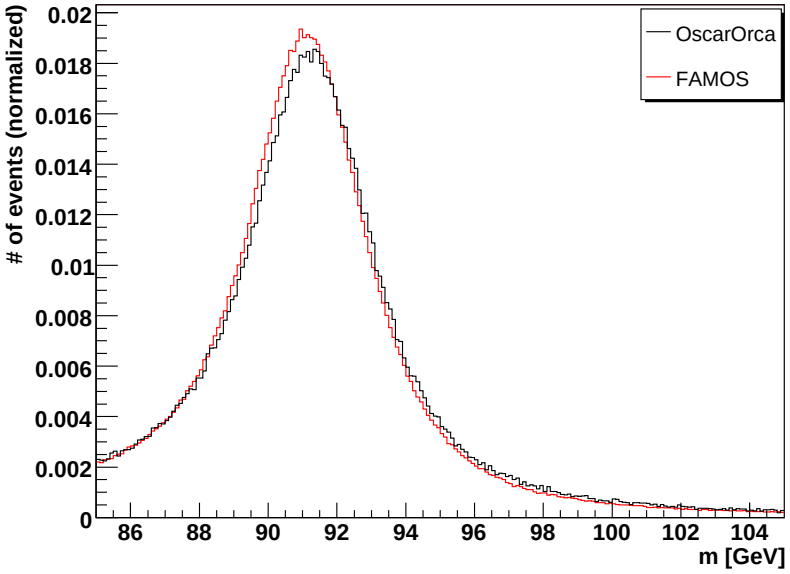

Figure 5: Comparison of reconstructed Z mass in FAMOS and OSCAR/ORCA. The red curve shows the OSCAR/ORCA distribution with a mean of $91.500{\pm}0.005$ GeV and a width of $3.055{\pm}0.003$ GeV. The FAMOS distribution, shown in black, has a mean of $91.339{\pm}0.002$ GeV and a width of $2.925{\pm}0.002$ GeV. The errors reflect the statistical precision of the available Monte Carlo samples.

the calorimeter towers. The effect of pile-up on the modelling of the transverse energy is quite important. Without the inclusion of pile-up in the fast simulation, the MET resolution is about 9 GeV, to be compared to 12 GeV from the full simulation with pile-up. The distributions of the missing transverse energy and the resolution on missing transverse energy are presented in Fig. 6, for the fast simulation with pile-up and for the full simulation with ORCA.

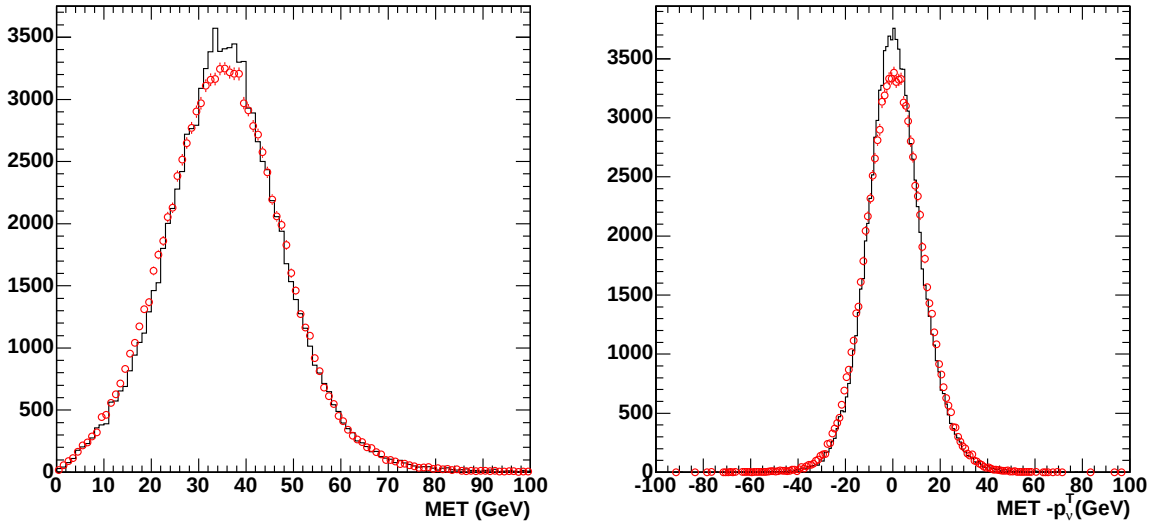

Figure 6: The missing transverse energy spectrum in $W \rightarrow e\nu$ events (left) and the missing transverse energy resolution (right). The distributions obtained with FAMOS with pile-up (solid line) and ORCA (open dots) are shown.

4 Measurements of the W mass from $W \to e\nu$ events

4.1 Event selections

Event selection are designed both to obtain a clean signal of $W \to e\nu$ events and a sample of $Z \to e^+e^-$ events that mimic at best the signal sample. $W \to e\nu$ candidates are selected among the events that passed the High Level Trigger (HLT) [9] for single leptons by requiring:

- one isolated electron with $E^T > 29$ GeV within the pseudo-rapidity region $|\eta| < 2.4$;
- missing transverse energy MET>25 GeV;
- transverse momentum $|\vec{u}|$ of the system recoiling against W has to be lower than 20 GeV, measured from the lepton p_T and the missing transverse energy;
- no jets in the event with p^T_{jet} >30 GeV.

The minimum accepted E^T is somewhat higher than the HLT single lepton threshold (26 GeV), to reduce the impact of a non uniform trigger efficiency near threshold, which is relevant when W events are compared to Z events (see below). The last two selections are intended to select W bosons produced with a small transverse momentum and to suppress background from QCD processes.

An additional selection on the electron pseudo-rapidity is introduced to avoid dead regions between the calorimeter modules ($1.10 < |\eta| < 1.68$), where the energy reconstruction is not optimal (see Fig. 7). The requirement on the electron to be in the fiducial volume leads to a loss of efficiency, but it is acceptable considering the high statistics available.

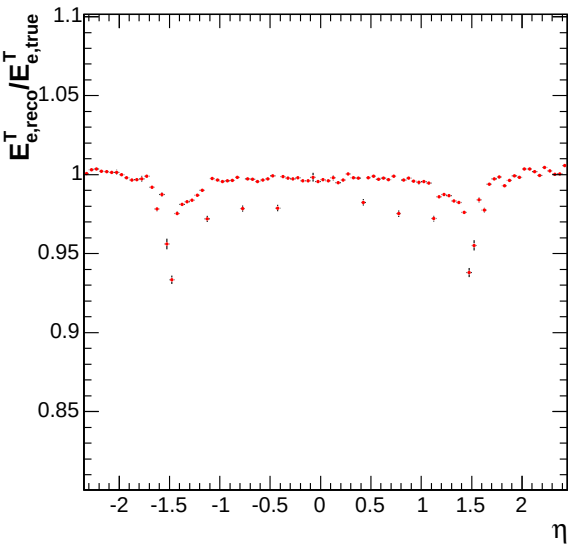

Figure 7: The ratio between the reconstructed transverse energy and the true transverse energy of the electrons in the W sample in function of the super-cluster pseudo-rapidity.

The selection efficiency is about 12.8% and the background contribution is at the 2% level, dominated by Z decays to leptons (see Fig. 8-left). The background in the W sample mainly consists of single electron events coming from $Z \to e^+e^-$ events with one electron escaping detection (1.3%) and from W and Z decays to τ's followed by a τ decay to an electron (1.2% and 0.2% respectively). We have tested the stability of these predictions against the assumptions in the Monte Carlo generator. A harder boson p^T spectrum would imply a higher efficiency of the E^T cut to electrons coming from tau decays. This is balanced by a lower efficiency of the requirement that the system recoiling against the boson be lower than 20 GeV. The final effect is at the 5% level for a p^T spectrum twice as hard as in the Monte Carlo generator, which is incompatible with existing data.

A contribution to the background can also be expected from di-jet events in which one jet mimics an electron and the other is mismeasured, creating missing E^T. Such events, referred to as QCD background, are contaminating the W samples collected at the Tevatron at the percent level or below [10]. At the LHC the production ratio of W to di-jet events of large p^T is somewhat less favourable than at the Tevatron and this background need to be controlled

carefully, as the uncertainty associated to it is larger than for the backgrounds mentioned above. A precise figure for the level of contamination due to QCD events could not be obtained with full detail, as a rejection power larger than 10^8 has to be established, which is beyond the statistical reach of the fast simulation. Still, a contamination lower than about 0.1% has been estimated as follows. "Fake-electron" from di-jet events are accepted by the single-electron HLT in a ratio 1:1 to $W \to e\nu$ events [9]. An additional reduction of the QCD background of order 10^3 is provided by the topological selections defining the $W \to e\nu$ sample. This has been verified by means of a sample of 10^6 di-jet events simulated with FAMOS, in which events with "quasi-electron" objects in the pseudo-rapidity region of $|\eta| < 2.4$ have been selected. "Quasi-electron" objects are defined as electron candidates (i.e. one super-cluster in the calorimeter linked to a track) failing at least one of the the electron definition criteria. This sagacity provides a sample of events statistically significant and with the same topological distribution as di-jet events with "fake-electrons". After applying the selection criteria for W events, no $W \to e\nu$ candidates were retained out of about 1000 events with "quasi-electron" objects, which implies a QCD background in the W sample at the 0.1% level or below. Noteworthily, this method can be applied to to directly estimate from real data themselves the level of background implied by QCD events (see also [10]).

Finally, the contribution from $b\bar{b}$ and $t\bar{t}$ production with either true or misidentified electrons in the final state are expected to be negligible, even in spite of large production cross sections. The former channel mainly provides electrons with small E^T to the beam axis, the latter is reduced by the requirements that no jets of large p^T be present.

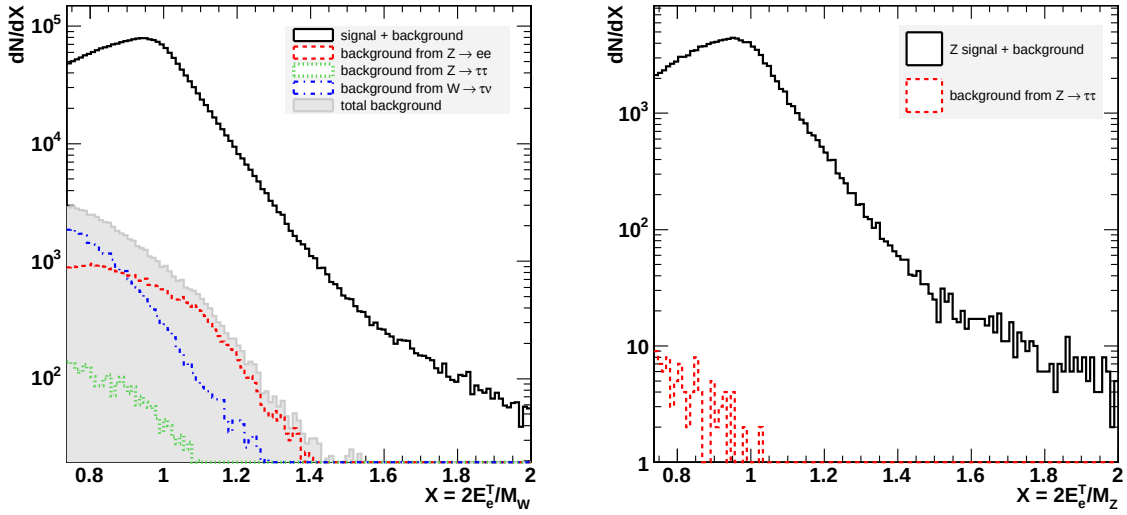

Figure 8: *Left:* The electron transverse momentum distribution in $W \to e\nu$ decays and the backgrounds from $Z \to e^+e^-$ (dashed line), from $Z \to \tau^+\tau^-$ (dotted line) and from $W \to \tau\nu$ (dot-dashed line) for 1 fb^{-1}. *Right:* The electron transverse momentum distribution in $Z \to e^+e^-$ events and the backgrounds from $Z \to \tau^+\tau^-$ (dashed line).

Z events used to predict the W spectrum are selected from the sample of events accepted by single lepton HLT. A Z/γ^* candidate event is tagged by requiring a pair of identified electrons in the region $|\eta| < 2.4$, with opposite charge and an invariant mass larger that 50 GeV. One of the two electrons, randomly chosen, is then removed from the event to mimic a W decay. The same selections discussed above are then applied, with the sagacity that the cut on the lepton quantities (minimum lepton E^T and event missing transverse energy) and on the momentum of the system recoiling against the W are scaled by the ratio M_Z/M_W. This choice is intended to minimise the difference in the acceptance to Z and W events and thus the theoretical uncertainties implied by the above mentioned approach. As for the W sample, a fiducial selection on the pseudo-rapidity of the electron retained in the Z events is applied[1)] The minimum E^T acceptance to electrons coming from Z decays is about 33 GeV, well above the single electron HLT threshold. The overall efficiency of these selections is about 7.4%.

The background in the Z sample is mainly due to $Z \to \tau\tau$ events with electron pairs in the final state and to W^+W^-, $c\bar{c}$, $b\bar{b}$ and $t\bar{t}$. For example, the background from $Z \to \tau\tau$ events, has been found to be at the 10^{-4} level

[1)] A similar restriction is not applied to the other electron, which is not directly used to predict the electron E^T spectrum from W decays, but is only needed to tag a Z event.

(see Fig. 8-right) and, in general, the total background is expected to be small. Moreover, it can be further reduced by testing the co-planarity of the electron pair.

A breakdown of the efficiency after each selection both for W and Z candidates is given in Table 4.1.

$W \to e\nu$		
Selection	number of events	% remaining events
no selections	1.75×10^7	100%
1 isolated HLT electron	6238091	35.6%
1 electron, $E_e^T > 29$ GeV	5475592	31.3%
MET$>$ 25 GeV	4564244	26.1%
$\vert\vec{u}\vert < 20$ GeV	3405938	19.5%
$p_{jet,max}^T < 30$ GeV	3117226	17.8%
electron in fiducial volume	2241893	12.8%
$Z \to e^+e^-$		
Selection	number of events	% remaining events
no selections	1.75×10^6	100%
2 isolated HLT electrons	424430	24.2%
1 electron, $E_e^T > 29$ GeV $\cdot M_Z/M_W$	301664	17.2%
MET$>$ 25 GeV$\cdot M_Z/M_W$	267501	15.3%
$\vert\vec{u}\vert < 20$ GeV$\cdot M_Z/M_W$	204353	11.7%
$p_{jet,max}^T < 30$ GeV	184117	10.5%
electron in fiducial volume	129273	7.4%

Table 1: Selection efficiencies for $W \to e\nu$ and $Z \to e^+e^-$.

4.2 Precision forecast

The study of the expected precision has been fully addressed for the analysis of the electron transverse energy spectrum with a statistical sample corresponding to 1 fb^{-1} of integrated luminosity. Some considerations about the achievable precision in the analysis of the transverse mass distribution are added at the end of this Section.

The evaluation of the systematic uncertainties of theoretical origin affecting the measurements is performed by determining the distortion to $R(X)$ implied by different effects affecting the theoretical prediction (PDF, Γ_W, perturbative expansion, ...) and by fitting the W event sample to Z events. The effects of instrumental origin have been studied by fixing $R(X)$ to the theoretical prediction exactly describing the samples of generated events (i.e. an exact knowledge of the theory is assumed) and by introducing distortions and biases in the detector response. The resulting shift in M_W, determined from a fitting procedure, is assumed as the systematic uncertainty associated to the effect. In this way systematics effects of instrumental origin and of theoretical origin are factorised.

A conservative figure for the uncertainties achievable with the first inverse femptobarn of integrated luminosity is assumed. Table 2 summarises our precision forecast and lists the effect considered, the required precision for 10 MeV shift in the W mass and the resulting error on M_W, given the level of precision that we expect to achieve. Extrapolation to 10 fb^{-1} are attempted when applicable. A detailed account of all the effects considered is given in the following. It might be already clear that the most critical effects are related to the definition of the lepton transverse energy scale and in particular to non-linearities in the scale, which are not cancelled in the ratio of W to Z events. On the other hand, the MET scale and the recoil model are only affecting the analysis through the event selection procedure and their impact on the measurement of the W mass is much diluted.

With the present knowledge, the largest systematic errors associated to this method may be of theoretical origin, related to the effects on the lepton transverse energy implied by the radiative corrections to the boson p^T spectrum.

4.2.1 Statistical method and precision

The analysis procedure is based on a χ^2 test of the compatibility of scaled transverse energy $X_T = 2E^T/M_V$ spectra of the electrons from Z- and W-boson decays. A statistical sample corresponding to an integrated luminosity of 1 fb^{-1} has been considered. In Z events, after scaling the transverse energy of one of the two leptons (randomly chosen) by $M_Z = 91.187$ GeV a weight to the event was attributed. The weighting function $R(X)$ can not be directly taken form the theory, but its shape must be determined from a detailed simulation to account for different acceptance and detector effects on W and Z events. This was accomplished by means of the FAMOS simulation,

Source of uncertainty	10 MeV effect on M_W	ΔM_W at 1 fb^{-1}	ΔM_W at 10 fb^{-1}
statistics		**40 MeV**	**15 MeV**
background	10%	10 MeV	2 MeV
electron energy scale	0.25%	10 MeV	2 MeV
scale linearity	0.00002 GeV^{-1}	30 MeV	<10 MeV
energy resolution	15%	5 MeV	2 MeV
MET scale	1.5%	15 MeV	<10 MeV
MET resolution	5%	9 MeV	< 5 MeV
recoil system	1.5%	15 MeV	<10 MeV
total instrumental		**40 MeV**	**<20 MeV**
PDF uncertainties		20 MeV	<10 MeV
Γ_W		15 MeV	<15 MeV
$p^T(W)$ spectrum		30 MeV	30 MeV (or NNLO)

Table 2: The columns list the effect considered, the required precision for 10 MeV shift in the W mass and the resulting error on M_W, given the expected level level of precision with first inverse femptobarn. In the last column, extrapolations to 10 fb^{-1}are attempted when applicable.

by using a statistical sample of Z events about ten times larger than in the simulated experiment, in order to have a negligible statistical inaccuracy in the determination of $R(X)$. The effect of the selection cuts applied sequentially to the simulated samples is illustrated in Fig. 9, where all the curves are normalised at $X_T = 1$.

The understanding of the effect of each selection on $R(X)$ is in order, as it was considered in the optimisation of the selection criteria. The selection on the invariant mass of the electron-positron pair is kept loose ($M_{e^+e^-}$ >50 GeV) on purpose as a corresponding selection can not be applied to the W sample. The selection on the pseudo-rapidity of the electron chosen to predict the E^T spectrum in W decays ($|\eta_1|$ <2.4) slightly distort $R(X)$ in the region with $X < 1$, because of the different rapidity distributions of the electrons in W and Z events. Being W^+ and W^- rapidity distributions different, the study of W^+ and W^- samples separately will provide a useful tool to understand and estimate possible systematic effects related to this aspect. More relevant is, instead, the cut on the pseudo-rapidity of the electron chosen to mimic the neutrino ($|\eta_2|$ <2.4) in Z events, which implies an unmatched selection between W and Z events. Low E^T electrons from the Z will have on the average an higher rapidity and therefore the cut on the rapidity of the second lepton mainly distort $R(X)$ in the low E^T region (that means low X_T). Finally, the requirement that $|\vec{u}|$, the transverse momentum of the system recoiling against the boson, be lower than a certain threshold has an effect on the tails of the X_T distribution, due to differences in the boson p^T spectra. The largest variations are anyway limited to the high X_T region and their impact can be reduced by properly restricting the fit range to the region $0.75 < X < 1.4$ around the Jacobian peak.

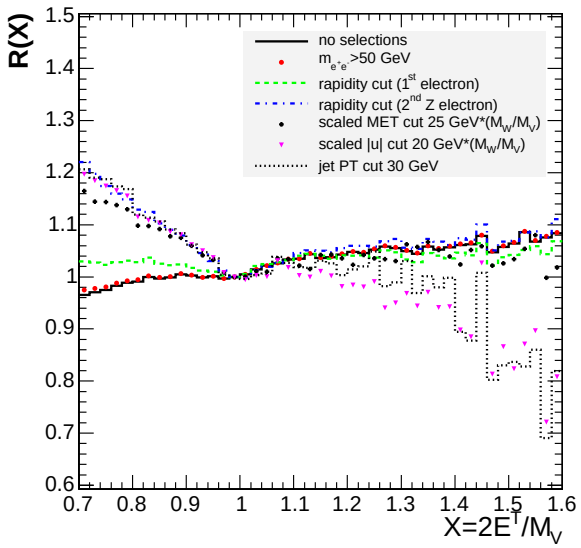

Figure 9: The re-weighting function $R(X)$ normalised where at $X = 1$ after event selection are sequentially applied applied to W and Z events.

In the fitting procedure, the transverse energy of electron candidates from W events is scaled to several different values of M_W and a χ^2 test of the two distribution is performed at each step. W- and Z-boson spectra are normalised in the fit range window. The χ^2 statistics reads:

$$\chi^2 = \sum_i \frac{\left(N_i^W(M_W)\frac{(N^Z R)_{tot}}{N_{tot}^W} - N_i^Z R_i\right)^2}{N_i^Z R(X_i)^2}, \tag{5}$$

where the sum is over the number of bins, N_i^W is the number of electrons from W decays in the i-th bin, $N_i^Z R_i$ is the number of

electrons from Z decays after proper rescaling through $R(X)$, $(N^Z R)_{tot}/N_{tot}^W$ is the relative normalisation of the spectra within the range considered in the fit. The term in the denominator only accounts for the statistical fluctuation on the number of Z events, as the relative contribution from W events is ten times lower and the statistical inaccuracy of $R(X)$ is also marginal. Events have been divided in approximately 1 GeV wide bins.

Figure 10-left shows the comparison of the electron X_T spectra for W- and Z-bosons at the best-fit point for a simulated statistics corresponding to 1 fb^{-1}of integrated luminosity. The χ^2 dependence on M_W is displayed in Fig. 10-right. The χ^2 was computed for a discrete set of M_W values and interpolated around the minimum with the quadratic: form $\chi^2 = \chi^2_{\rm min} + (M_W - M_W^{\rm best})^2/\Delta M_W^2$. A statistical precision of about 40 MeV, limited by the quantity of Z events, is obtained. The smearing of the Jacobian peak in the lepton E^T spectrum is dominated by the finite boson p^T. The statistical precision would worsen to 50 MeV, if the boson p^T spectrum was about 30% harder than predicted by the current Monte Carlo. Extrapolation to 10 fb^{-1} of integrated luminosity readily results in a statistical precision of less than about 15 MeV.

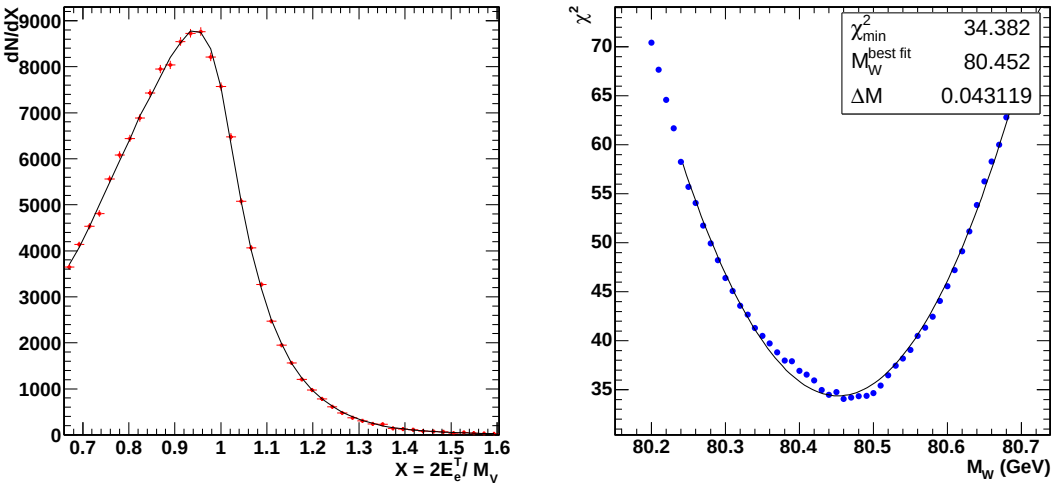

Figure 10: Comparison of the scaled electron E^T spectra for Z- (dots) and W-boson (line) events (left) and χ^2 dependence on M_W for 1 fb^{-1} integrated luminosity (right).

4.2.2 Systematic uncertainties of instrumental origin

The final precision on M_W will be affected by several systematic uncertainties of instrumental origin. Hereafter the main effects are considered along with the methods to control them. The precision expected from the first sample of 1 fb^{-1} and the final sample of 10 fb^{-1} of data collected during the low luminosity phase are quoted.

Background modelling: In the method proposed there are two sources of backgrounds that need to be kept under control: the background in the $W \to e\nu$ sample and the background in the Z sample. The former requires a precise modelling and needs to be added to the Z scaled sample in the fitting procedure. The latter is dangerous as it could spoils the reliability of the Z to W scaling procedure. Yet, as discussed in section 4.1, it is expected to be small.

Background samples corresponding to 1 fb^{-1} of integrated luminosity for the processes $Z \to e^+e^-$, $Z \to \tau^+\tau^-$, $W \to \tau\nu$ have been generated and processed with the FAMOS simulation. Events surviving the selection criteria

have been added to the $W \to e\nu$ candidate sample. The same background model was also added to the sample of scaled Z events entering the fitting procedure. In the latter case, the relative normalisation of the background has been assumed to be uncertain and the best fit value for M_W has been extracted for several different background normalisations. The variation of M_W determined form the fitting procedure as a function of the background normalisation is shown in Fig. 11, indicating that a precision of around 1 MeV would require a background knowledge at the 1% level.

Assuming the background to be known at the 10% level as in the CDF experiment [10], we can foresee an uncertainty of the order of 10 MeV on the W mass. This is a conservative figure for the initial phase, as most of the uncertainty in the background modelling is related to the QCD background, which is expected to be smaller at the LHC than it was at the Tevatron (see Section 4.1). Moreover, the use of di-jet events with "quasi-electron" objects and a topology similar to $W \to e\nu$ decays will enable a good modelling of this background from the data themselves. A systematic uncertainty below 5 MeV on the W mass can be anticipated for the final analysis with 10 fb^{-1} of integrated luminosity.

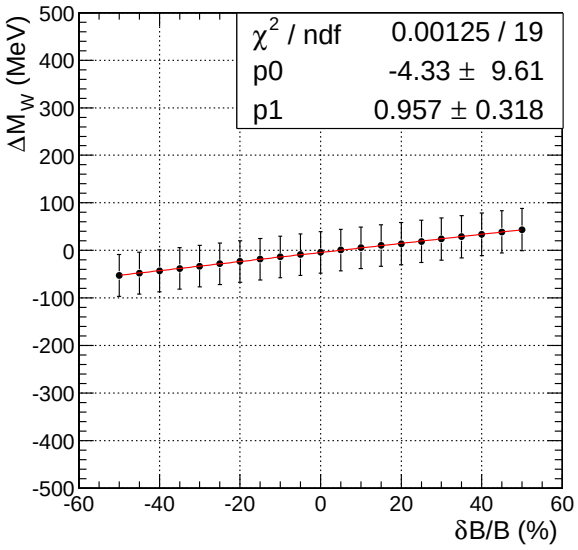

Figure 11: The shift ΔM_W as a function of the uncertainty $\delta B/B$ in the total background normalisation.

Trigger and selection efficiency: Trigger and selection efficiency are relevant because they induce distortions to the $R(X)$ theoretical prediction that need to be corrected for.

At the trigger level a selection of single electron events with a transverse energy E^T threshold of 26 GeV is applied. The observable relevant to this analysis is not directly E^T, but the scaled variable $2E^T/M_V$. A threshold at $X_T = 0.75$ is applied in the analysis, corresponding to about 30 (33) GeV for electrons coming from the W (Z) decay. At these energies the trigger efficiency is already independent of the transverse energy [9]. A possible residual dependence can be established through the analysis of $Z \to ee$ events triggered by the double-electron HLT and compensated for in the definition of $R(X)$ the final effect on M_W is expected to be small.

In order to quantify an uncertainty associated to the selection criteria, each selection cut has been moved by an amount corresponding to the resolution and the scale uncertainty anticipated for the observable under consideration. The re-weighting function was not changed, instead. This procedure describes a possible mismatch between the final experiment and the Monte Carlo which is assumed to describe it and to provide $R(X)$. The variation of the selection cut on the observables with a good resolution has a marginal impact on M_W. This is true for all the observables, but the missing transverse energy (MET) and the transverse momentum of the recoil system ($|\vec{u}|$), which are considered in more detail in section 4.2.2

Electron energy calibration: The energy scale can be modified in two ways: by an absolute scale factor and by a non linearity term. The effect of the former mis-calibration is expected to be largely reduced by the adopted analysis strategy, as a common mis-calibration in Z and W events will cancel in the ratio. The latter effect is more nasty.

Absolute scale calibration: The impact of the uncertainty on the electron energy scale has been estimated introducing a mis-calibration factor $\delta E^T/E^T$ on the reconstructed transverse energy of the lepton, both in the W and Z samples.

In Fig. 12, the shift on the W mass extracted from the fitting procedures shown as a function of the applied mis-calibration factor. A shift ΔM_W of about 40 MeV for $\delta E^T/E^T$ $\sim$1% is found. This is about 20 times smaller than the impact of the scale uncertainty in the traditional approach. Ideally, in the method adopted, the effect of a scale uncertainty should be exactly zero, the residual effect is due to the slope of the re-weighting function: a wrong scale results in a wrong weight.

The statistical precision on the overall energy scale with 1fb^{-1} is expected to about 0.05% from the calibration of the electromagnetic calorimeter using $Z \to e^+e^-$ events [11]. Non-uniformities in the response to electrons as a function of η are expected, as a result of the variation of the tracker material distribution in front of the calorimeter. These would spoil the resolution and not the overall scale. Nevertheless, we have conservatively assumed that the energy scale be known with a precision of 0.25% in the initial phase. This figure, comparable to the precision of the calorimeter inter-calibration, would lead to an uncertainty on W mass measurement of about 10 MeV, that is anyway marginal with respect to the statistical precision of the method.

The estimate of the transverse energy of the electron is based on the calorimetric measurement of the energy and on the measurement of the θ direction from the tracker. The major impact on the W mass precision is expected to come from the energy scale measured in the electromagnetic calorimeter. The measurement of the θ direction is not critical and the precision available in the first run will suffice. The uncertainties on the magnetic field mapping, relevant in the bending plane, are not of direct importance in this measurement.

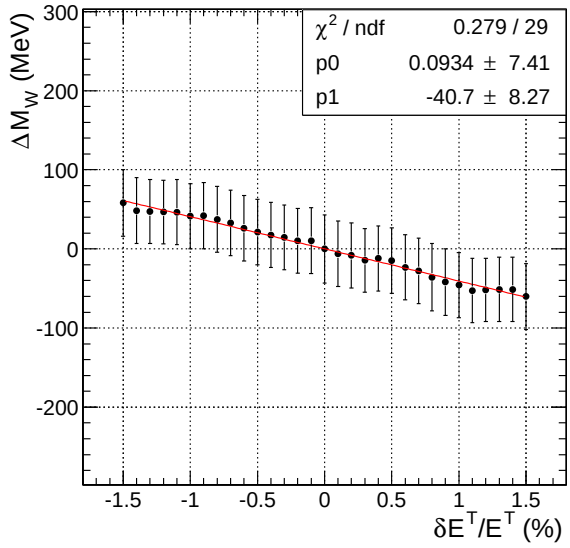

Figure 12: The shift ΔM_W as a function of the relative mis-calibration factor $\delta E^T/E^T$ in the transverse energy scale.

Energy scale non-linearities: The effect of non-linearities in the estimate of the transverse energy, which are expected to be present, are definitely more critical. The prediction of the transverse spectrum for the observable $X_T = 2E^T/M_W$ is based on a scaling procedure from a corresponding variable in the Z events. Due to the 10% mass difference between the two vector bosons, a 10% difference in the range of E^T spectra relevant in the two cases is anticipated. A non-linearity in the energy scale about the Jacobian peak can be parameterised as:

$$E^{T\prime} = E^T(1 + \epsilon(E^T - \frac{M_Z}{2})) \tag{6}$$

While this results, on the average, in a correct transverse energy estimate for Z events, a shift in the transverse energy estimate for events around the Jacobian peak of the W boson is expected:

$$\delta_{E^T} \sim \frac{1}{4} M_W \epsilon (M_W - M_Z) \tag{7}$$

This implies a shift in the determination of the W mass of around $2\delta_{E^T}$, which is of order of 10 MeV for a non-linearity of 2×10^{-5} GeV^{-1}. This rough estimate, well consistent with the required precision quoted by the CDF

experiment [10], has been confirmed by changing the non-linearity in the computation of $R(X)$, while leaving unaffected the sample simulating the experiment. Any differential non-linearity between the Monte Carlo and the final experiment will therefore need to be controlled at this level. This is a serious challenge, since the methods used at the Tevatron to control non-linearities will not be easily available. In particular, the Υ and J/ψ resonances will be largely filtered by the single- and double-electron HLT and in any case will provide mostly events of low transverse energy. On the other hand, the control of the linearity based on a comparison of the momentum to the energy scale, also attempted at Tevatron, is also difficult and would bring magnet and tracking uncertainties into the game. This is not desirable in particular with the first sample of collected data. To cope with these difficulties and limitations, a different procedure is envisaged, based on the use of $Z \to ee$ events alone. The invariant mass of an e^+e^- pair is indeed modified (twice) by the same non-linearity factor entering equation (6). This can be measured by looking at the distribution of the average value of $\log(Q^2/M_Z^2)$ as a function of the E^T of one of the two electrons of the Drell-Yan pair. This distribution is expected to be a linear function of E^T with slope ϵ and a possible offset given by the absolute energy scale. Indeed, a mis-calibrated and non-linear energy response would result in a squared invariant mass Q'^2 given by:

$$< \log(Q'^2/M^2) > = < \log(Q^2/M_Z^2) > + \log(1+s_E) + \log(1+\epsilon\Delta E_1^T) + \log(1+\epsilon\Delta E_2^T) \quad (8)$$

$$\sim < \log(Q^2/M_Z^2) > + s_E + \epsilon\Delta E_1^T + \epsilon\Delta E_2^T \quad (9)$$

where, the second equality holds upon the condition that the absolute scale mis-calibration (s_E) and the non-linearity terms be small. Differential non-linearities$\xi = \Delta\epsilon$ between the data and the Monte Carlo simulation used to define the re-weighting function will then manifest themselves as

$$\Delta(< \log(Q'^2/M^2) >) \sim \Delta s_E + \xi\Delta E_1^T + \xi\Delta E_2^T \quad (10)$$

Moreover, if only the dependence on either of the two lepton E^T is considered, the effect of the other averages out. The application of this method is shown in Fig. 13, where events passing the double-electron HLT have been considered, with the additional requirement that the two electrons be within the rapidity acceptance of the analysis and that $|E_1^T - E_2^T| < 30$ GeV. The latter condition corresponds to the requirement of a Z candidate with small transverse momentum. These events well describe the kinematic region of events considered in the W mass analysis. Non-linearities in the response to the electrons are expected to be rapidity dependent, due to the variation of tracker material, and can be studied by dividing the $Z \to ee$ sample into several rapidity bins. To test the method, differential non linearities of ± 0.0002 GeV^{-1} have been artificially introduced in the simulation and are correctly extracted from a linear fit to the distribution, with about 2×10^{-5} GeV^{-1} statistical precision [2)]. This figure can be contrasted to the systematic limitation of about 6×10^{-5} GeV^{-1} quoted by the CDF experiment [10], based on the comparison of the energy and the momentum scales, and implies an estimated uncertainty of 10 MeV on the W mass. Should one keep the CDF value as the initial estimate of the differential non-linearities in the data and Monte Carlo, an uncertainty of around 30 MeV on the W mass would be obtained.

At 10 fb^{-1} when larger statistical samples will be available and a better understanding of the overall detector response including tracking will be gained, the method proposed here can be cross-checked with more traditional approaches to help reduce the uncertainty below 10 MeV.

Electron energy resolution: Even if the resolution on the transverse energy of the electron is better with respect to the one of the transverse mass, it can't be neglected in the definition of $R(X)$. Figure 14 shows, as an example, the ratio between $R(X)$ obtained with transverse energy of the electron at the generator level and $R(X)$ computed from the reconstructed E_e^T: the presence of a slope, though marginal, suggests that if the resolution is not account properly in the computation of $R(X)$, Z events are wrongly weighted leading to a shift in the W mass.

The study of resolution effects has been performed modifying the width of the E_e^T resolution in the W and Z samples, keeping its shape fixed. The fitting procedure was then repeated for different values of the resolution using the weighting function of par. 4.2.1. In Fig. 15 the variation of the W mass value obtained from the fit is plotted as a function of the relative change in the transverse energy resolution. The knowledge of this resolution with a relative accuracy of 1%, would give an uncertainty below 1 MeV on the W mass.

The energy resolution can be measured from the measured width of the Z line shape. The CDF experiment measured it with a precision of about 10%, limited by the Z statistics, while a systematic limitation of 1.5%,

[2)] Noteworthily, according to the simulation a non-linearity of about 1.4×10^{-4} GeV^{-1} is estimated from the direct comparison of the electron E^T at the generator level and after reconstruction. The same value is also retrived by the outlined method, by comparing the distributions at the generator level and after reconstruction.

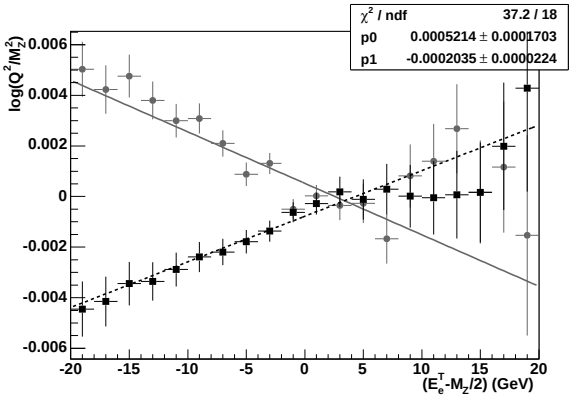

Figure 13: Dependence of $\Delta(< \log(Q^2/M_Z^2) >)$ as a function of the E^T of one of the two electrons of a Drell-Yan pair. The default FAMOS simulation is taken as a reference and compared to simulated data samples where additional non-linearities of ± 0.0002 GeV^{-1} have been introduced. The effect of the differential non-linearity is evident in the slope of the distribution.

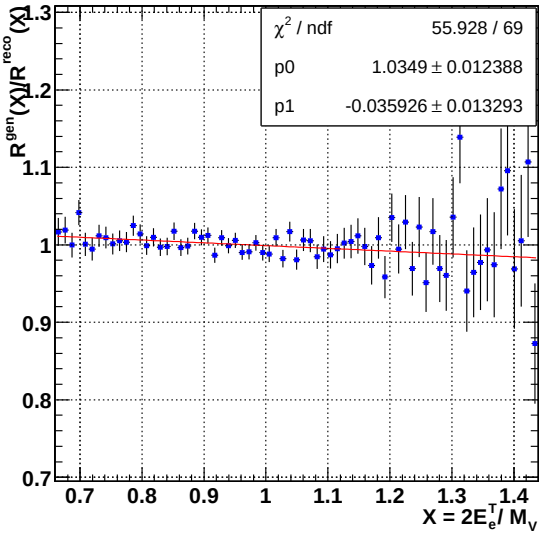

Figure 14: The ratio between the re-weighting function R^{gen}(X) computed using E_e^T at the generator level and R^{reco}(X) from the reconstructed variable.

related to photon radiation from the final state electrons, was claimed. At the LHC the statistical error will be nearly negligible and the knowledge of the resolution will be dominated by systematic effects. Lacking at this very moment any detailed study on the resolution modelling for the CMS detector through the analysis of the Z line shape, we conservatively assume an initial uncertainty of 5 MeV on the W mass, corresponding to a relative uncertainty of about 8% on the transverse energy resolution.

MET scale and recoil model The knowledge of the MET scale and resolution as well as the detailed modelling of the underlying event is not as critical in the analysis of the electron E^T as in the reconstruction of the transverse mass observable. Their effects are only indirectly entering in the selection procedure and are not directly affecting the variable considered to extract M_W. Thus, their contribution to the total uncertainty on M_W is expected to be smaller than the systematic contributions discussed above.

These contributions have been evaluated by fixing the $R(X)$ to be used in the scaling procedure to the one obtained from our standard set of selection cuts, and by repeating the fitting procedure on simulated experiments with W and Z samples selected with modified cuts on MET and $|\vec{u}|$. The result is a shift in the W mass of around 8 MeV for 1% uncertainty on the MET scale and for 1% uncertainty on $|\vec{u}|$.

The MET scale and the MET resolution can be studied, and possibly tuned, using $Z \to ee$ events in which either

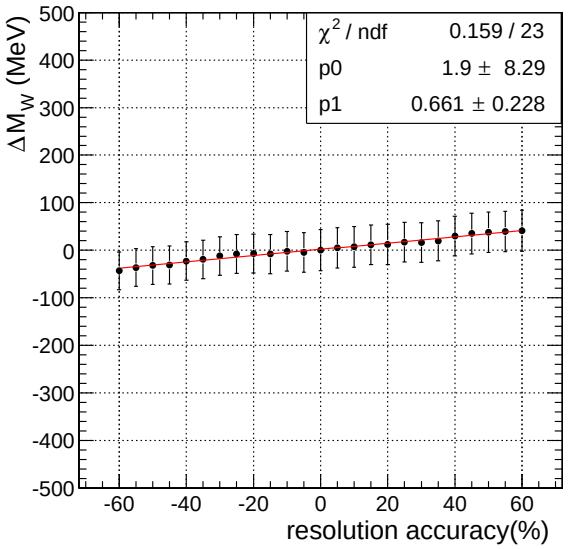

Figure 15: The shift ΔM_W as a function of the accuracy on the resolution of transverse energy scale.

of the two leptons is suppressed. In such events, we define $\widetilde{MET}$ as the sum, with opposite sign, of the transverse energies of all the calorimeters towers, but those corresponding to the killed lepton. $\widetilde{MET}$ has to be compared to the transverse energy $E^T_{e,suppressed}$, which is well measured in the electromagnetic calorimeter, in order to check the MET scale and resolution.

Some restrictions are to be considered when transporting this calibration to W events, because of two reasons. Firstly, at variance with W decays, where true missing energy is present, in $Z \to ee$ events one lepton need to be suppressed and its hits completely removed in the computation of $\widetilde{MET}$. Moreover, the underlying event in Z and W boson production is expected to be different. Thus, systematic limitations arise in the achievable precision of the MET calibration as shown illustrated in Fig. 16. On the left, the mean value of the one transverse component[3)] of $\widetilde{MET}$ from $Z \to ee$ is plotted as a function of the same component of the transverse energy of the electron removed from the MET computation; on the right one component of the MET in $W \to e\nu$ events is plotted versus the same component of the neutrino momentum at the generator level. The comparison is restricted to a momentum region corresponding to the same kinematic region for Z and W decays. A difference of about 1% in the slopes is observed, this is consistent with the 1.5% effect observed in a similar study with muon events. A figure of 2% is taken as a conservative estimate of the systematic uncertainty on the MET scale achievable with the first 1 fb^{-1} of collected data, giving a contribution of about 15 MeV on the W mass. Noteworthily, either slope is determined with a far better precision, implying that this uncertainty could be reduced.

The MET resolution can be monitored similarly. Figure 17-left shows the resolution $\widetilde{MET}_x - E^T_{e,x}$ on the MET estimate in $Z \to ee$ events: a width of around 9.6 GeV is obtained from a Gaussian fit to the distribution. This can be contrasted to a resolution $MET_x - p_{\nu,x}$ of about 9.2 GeV obtained in $W \to e\nu$ events (Fig. 17-right). As a cross check, the same analysis has been repeated on a sample of simulated events without pile-up and a resolution of 8.4 GeV and 8.0 GeV has been obtained for the MET components in Z and W events respectively. It follows that the observed difference can not be ascribed to pile-up events, which consistently worsen the resolution by about 4.5 GeV in quadrature in both samples. The full difference, amounting to 5% relative, is taken as a preliminary estimate of the systematic uncertainty on the MET resolution. The impact of this effect on the W mass has been evaluated by selecting W and Z candidates from samples with a MET resolution worsened by 5% and by repeating the fitting procedure while keeping unchanged $R(X)$. A shift in the W mass of about 9 MeV is observed and is taken as an estimate of the systematic error.

A similar study can be performed to control the transverse momentum $|\vec{u}|$ of the hadron system recoiling against the boson. In this case, the control can be performed using the hadron recoil to the Z boson in a sample of $Z \to ee$ events. In these events, $|\vec{u}|$, defined as the sum of all the hits in the calorimeters after removing the ones associated to the two electrons, can be compared to the P^T of the Z boson, which is reconstructed with good precision from the two electrons.

[3)] Namely the x-component.

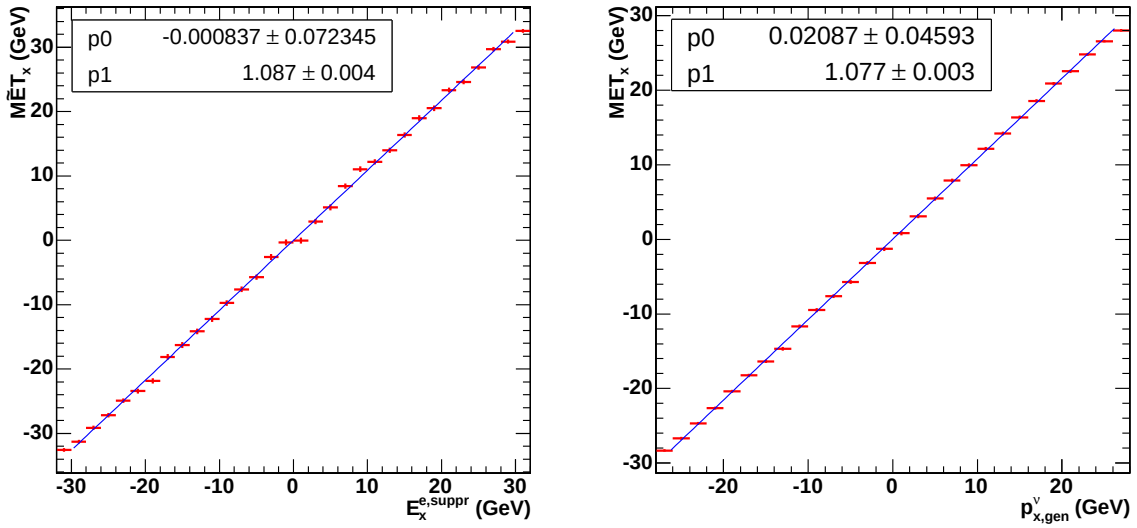

Figure 16: The x component of the $\widetilde{MET}$ from $Z \to ee$ events as a function of the x component of the energy of the suppressed lepton in the range between -30 GeV and + 30 GeV (left); the slope is 1.087±0.004. The x component of the reconstructed MET as a function of the $p_{\nu,x}$ in $W \to e\nu$ events is shown on the right; the slope is 1.077±0.003.

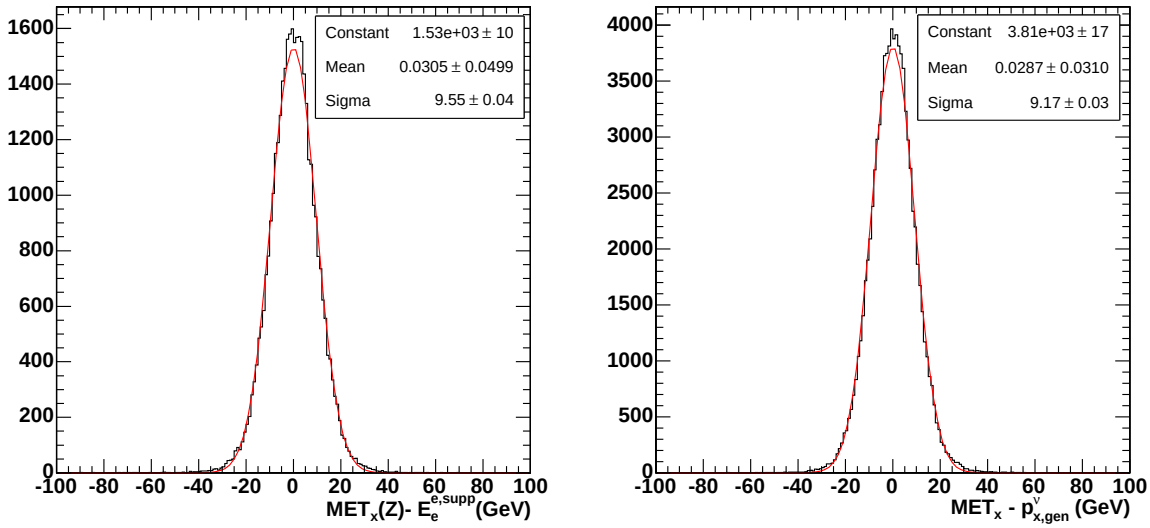

Figure 17: The distribution of $\widetilde{MET}_x - E_{e,x}^T$ obtained in $Z \to ee$ events with one lepton suppressed (on the left) and the distribution $MET_x - p_{\nu,x}$ in $W \to e\nu$ events (on the right). The resolution on each MET component extracted from $Z \to ee$ events is 9.6 GeV, the resolution in $W \to e\nu$ is 9.2 GeV.

The systematic effect related to this procedure has been estimated by computing the difference in the slopes of the u_x^Z versus P_x^Z distribution and the u_x^W versus P_x^W taken at the generator level. The effect is at the level of 2% and leads to an uncertainty in W mass of about 15 MeV.

4.2.3 Systematic effects of theoretical origin

PDF uncertainties Different Parton Distribution Functions (PDF) are implied in the hard scattering processes for W and Z production. The limited knowledge of the PDF involved in the W and Z production is then determining an uncertainty on the acceptance and on the differential distributions predicted for W- and Z-boson events. Eventually, in the context of the method discussed here, these effects are best represented by looking at the distortion induced on $R(X)$ by the uncertainty on the PDF parameters. An example of these distortions is shown in Fig. 18 for some sets of PDF of the CTEQ61 [12] and MRST [13, 14, 15] families. These were computed by

means of the LHAPDF libraries [16] to re-weight the simulated data samples.

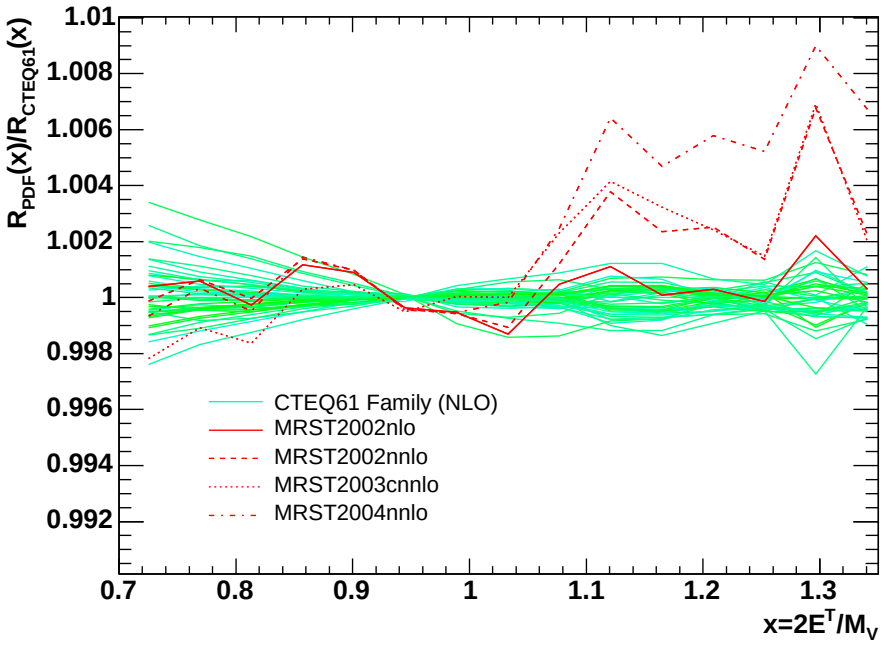

Figure 18: Ratio of $R(X)$ as a function of $X = 2E^T/M_V$ for several different sets of PDF's to the $R(X)$ computed for the central value of the CTEQ61 PDF set.

The impact on the determination of M_W can then be determined quantitatively by repeating the fitting procedure for several re-weighting functions $R(X)$, corresponding to different PDF parameters' sets and by determining the effect on M_W. In this procedure we have mainly considered the PDF set CTEQ61[12]. According to the PST approach [17], this PDF family contains one central PDF set ($i = 0$) and 40 PDF members, $F^{\pm} = F(x, Q; s_i^{\pm})$ $(i = 1, 20)$, representing the PDF variations induced by a change of ± 1 sigma of each independent parameter describing the PDF set. The master equation proposed by Nadolsky and Sullivan [18] is used to determine the effect on M_W:

$$\Delta M_W^+ = \sqrt{\sum_{i=1}^{20} \left[\max\left(M_W(s_i^+) - M_W(0), M_W(s_i^-) - M_W(0), 0\right)\right]^2} \tag{11}$$

$$\Delta M_W^- = \sqrt{\sum_{i=1}^{20} \left[\max\left(M_W(0) - M_W(s_i^+), M_W(0) - M_W(s_i^-), 0\right)\right]^2} \tag{12}$$

where $M_W(s_i^{\pm})$ represent the best-fit value for the W mass corresponding to the PDF set under consideration.

Figure 19 shows the quantities $\Delta M_W(s_i^{\pm}) = M_W(s_i^{\pm}) - M_W(0)$ as determined by the fitting procedure using the 40 different members of the CTEQ61 family to determine $R(X)$. The largest variations are of order 10 MeV and correspond to CTEQ61 members implying a large distortion of $R(X)$ in the low X_T region, where most of the events lie. The resulting uncertainty on m_W is:

$$\Delta m_W^+ = 23 \text{ MeV} \tag{13}$$

$$\Delta m_W^- = 17 \text{ MeV} \tag{14}$$

These figures can be quoted as the expected systematic error coming from PDF uncertainties, as the PDF sets belonging to the MSRT family at NLO and NNLO give results consistent to the CTEQ61 central value within 10 MeV. The largest differences on $R(X)$ between the CTEQ61 and the MRST sets are indeed limited to the region of large X_T (see Fig. 18).

It must be noted that early LHC results will definitely imply an improved determination of the PDF sets relevant to this analysis. Hence, the figures quoted above have to be regarded as a conservative estimate of the uncertainty induced on M_W for an integrated luminosity of 1 fb^{-1}, while a substantial reduction of this error is expected at increased luminosities.

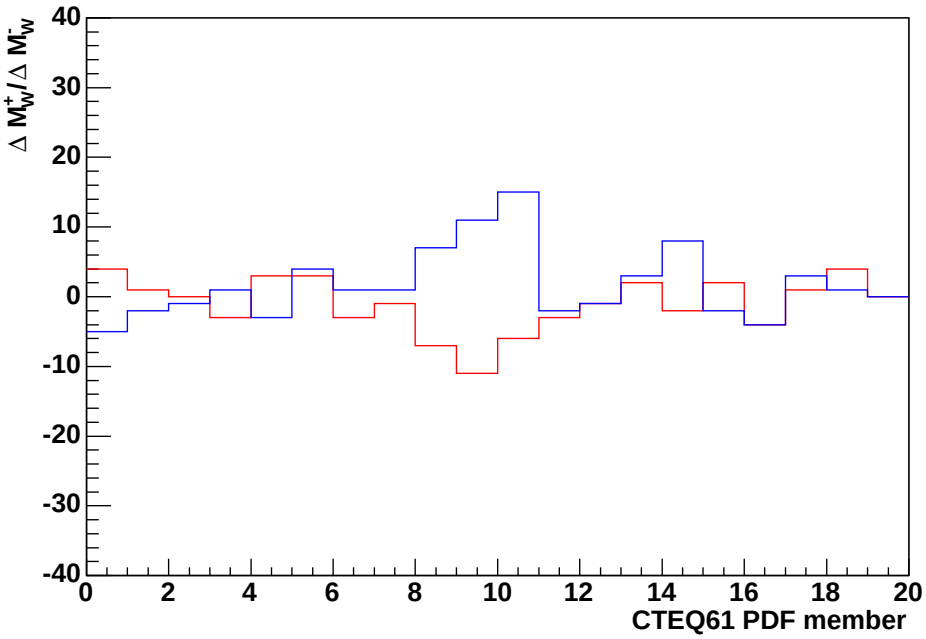

Figure 19: $\Delta M_W(s_i^{\pm}) = M_W(s_i^{\pm}) - M_W(0)$ as determined by the fitting procedure using the 40 different members of the CTEQ61 family to determine $R(X)$.

Effect of Γ_W The present uncertainty on Γ_W is of about 30 MeV from direct measurements and somewhat better from the indirect constraints assuming Standard Model consistency. Such a variation of Γ_W would directly affect the shape of the Jacobian peak and modify the high E^T tail of the transverse energy distribution. This can be exploited in a two-parameter fit of the observed distribution, which has not been attempted yet. We have preliminary tested, instead, the uncertainty induced on the W mass, assuming an uncertainty of 30 MeV on Γ_W, which can be accounted for in our procedure by modifying $R(X)$ accordingly. As discussed in [4], a change in Γ_W results in a variation of the Z to W normalisation (the $R(X)$ shape) above the resonance ($X_T > 1$), while leaving unaffected the normalisation below the resonance. An uncertainty of 30 MeV in Γ_W translates in a normalisation uncertainty above the resonance of about 0.5%, which correponds to an uncertainty of about 15 MeV on the W mass.

$p^T(W)$ spectrum The measurement of the W mass through the analysis of the lepton transverse energy distribution is directly affected by the uncertain knowledge of the $p^T(W)$ distribution. In the context of the method discussed, this uncertainty is better quantified as the uncertainty associated to the theoretical prediction of $R(X)$ for $X_T = 2E^T/M_V$ due to soft gluon emission. These uncertainties are largely cancelled in the ratio, but unlike for the scaled transverse mass distributions, the cancellation is not complete. A comparison of the available calculations at the NLO to the LO in α_S shows a difference of up to 10% in the ratio in the region above the resonance ($X_T > 1$). A preliminary estimate of the error associated to the missing orders in the perturbative expansion has been addressed by studying the dependence of the NLO prediction on the choice of the renormalisation and factorisation scales. The computation has been performed with the DYRAD program [19], which also allows for the introduction of experimental selections (lepton transverse energy and rapidity, missing energy and leading jet energy). A reference point has been computed with the renormalisation and factorisation scales both set to the boson mass ($M_V; V = W, Z$): a natural scale of the process under study. Test points have been calculated by changing either scale and both to $0.5M_V$ and $2M_V$. Our results are summarised in Fig. 20, which shows the ratio of $R(X)$ as a function of $X = 2E^T/M_V$ for different choices of the scales to our reference $R(X)$. Shape variation at the 1% level are observed in the region relevant to the fitting procedure ($0.75 < X_T < 1.35$), although the numerical (statistical) precision of the computation is not optimal. These distortions have been propagated to the fitting procedure and shifts in the W mass up to 30 MeV are observed. This is our preliminary estimate of the systematic uncertainty on the W mass implied by the uncertain knowledge of QCD radiative corrections ($p^T(W)$ spectrum in Table 2). A more detailed analysis, with improved numerical precision is in order to quantify the ultimate precision of this method at 10 fb^{-1} of integrated luminosity. Should the precision turn out to be insufficient, the extension of the calculation one order higher in α_S is technically feasible [4].

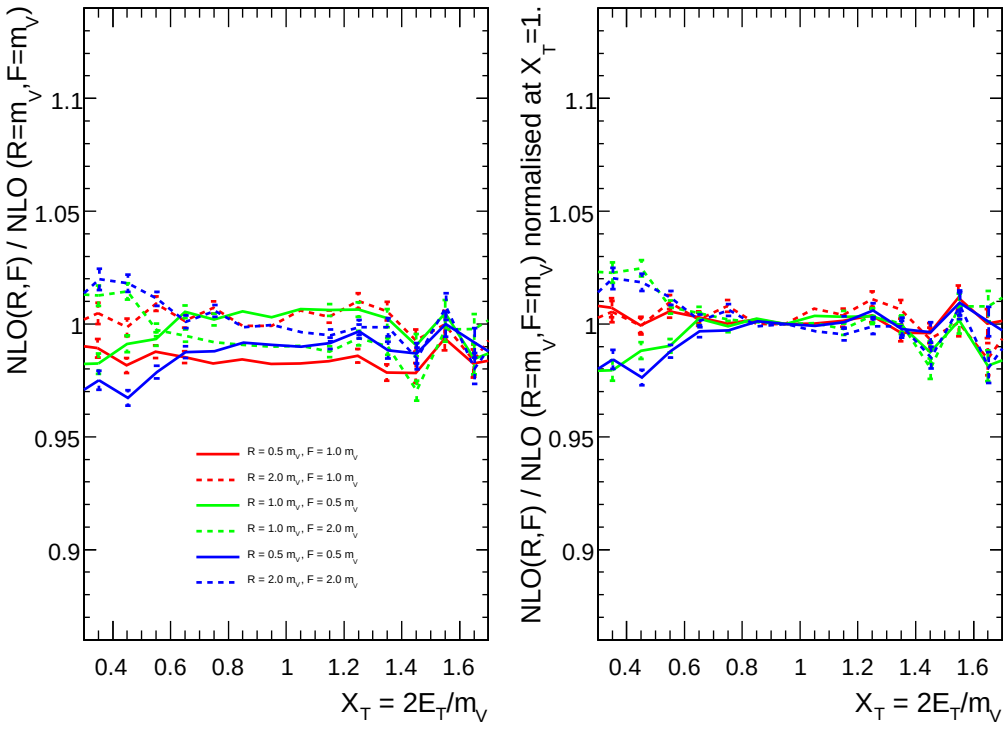

Figure 20: Ratio of $R(X)$ as a function of $X = 2E^T/M_V$ for different choices of the renormalisation (R) and factorisation (F) scales to our reference $R(X)$ computed with $R = M_V$ and $F = M_V$. In the left panel, all the curves are normalised at $X = 1$ to put in evidence shape variations. The error bars indicate the numerical precision of the computation.

4.2.4 Measurement of M_W from the scaled transverse mass spectrum

The theoretical limitation discussed above is marginal in the analysis of the scaled transverse mass ($X_{m^T} = m^T/M_V$) distributions. In this case, indeed, $R(X_{m^T})$ is stable against radiative corrections [4].

The analysis of this observable has not been addressed in detail. On the other hand, most of the systematic limitations of instrumental origin are expected to be similar to the one discussed in the next Section for the analysis of $W \to \mu\nu$ events. The statistical precision has been tested to be about 50 MeV at 1 fb^{-1} of integrated luminosity. This figure is somewhat worse than in the analysis of the electron E^T as the resolution on the transverse mass is worse, although similar (see Fig. 1).

5 Measurement of the W mass from $W \to \mu\nu$ decays

5.1 Event Selection

The following subsections describe the selection of W and Z events.

5.1.1 Detector Acceptance and Trigger System

The Level-1 trigger accepts only single muon events with a transverse momentum of the muon greater than 14 GeV. For di-muon events the threshold is lowered to 3 GeV for each muon. The High Level Trigger enforces these constraints to 19 GeV for a single muon event and 7 GeV for di-muons, respectively. An overview of the trigger acceptance is given in Table 3.

	single muon events	di-muon events
Level-1 trigger	14 GeV	3 GeV; 3 GeV
High Level Trigger	19 GeV	7 GeV; 7 GeV

Table 3: Overview of the muon acceptance of the CMS Trigger System. The thresholds are given for single muon and di-muon events as these are characteristic for muonic W and Z boson decays [20].

In addition, effective muon reconstruction is only possible in the barrel region and the endcaps of the CMS detector. These areas cover values in pseudo-rapidity up to $|\eta| \leq 2.4$. The selection cuts for the analysis are chosen tighter than the constraints of the detector and the trigger system in order to avoid threshold and edge effects.

5.1.2 Z Boson Event Selection

In order to achieve a clean Z sample, the following selection cuts are applied. Two isolated muons are required with transverse momenta $p^T \geq \frac{M_Z}{M_W} \cdot 25$ GeV and within a pseudo-rapidity range of $|\eta| \leq 2.3$. The transverse momentum of the boson is balanced by the hadronic system recoiling against it. Only events satisfying an hadronic recoil $\vec{u}$ with $|\vec{u}| \leq 20$ GeV are selected. The recoil is determined from the missing transverse energy measured in the calorimeter. Events with at least one extra jet with $p^T_{jet} \geq 30$ GeV or with more than one jet are also discarded. These cuts also suppress the QCD background. A summary of the applied selection cuts and the fraction of remaining Z boson events after each cut is presented in Table 4.

After these cuts, a very clean sample of Z boson events is expected, containing only an irreducible, but well predicted fraction of Drell-Yan events produced through a virtual photon. This conclusion is supported by current results by the the Tevatron experiments CDF and DØ, who observe no significant contribution of background processes to their Z signal [21].

Possible background processes to the channel $Z \to \mu^+\mu^-$ have been generated with PYTHIA with the constraint that only events with two or more muons are selected. In addition, it is required that the transverse momentum of each muon is larger than 25 GeV and that their pseudo-rapidity fulfils $|\eta| \leq 2.4$. Having found an event that has passed these preselection cuts, the invariant Z mass is reconstructed considering the following criteria: the two muons have opposite charge and the combination with the invariant mass closest to the Z mass is selected. The results of the different processes are compared with the number of signal events corresponding to an integrated luminosity of 287 pb^{-1}. These 465 000 $\mu^+\mu^-$ events are reduced by the selection cuts to a total of 154538.

A possible background candidate is the process $pp \to b\bar{b} \to \mu^+\mu^- + X$ with a decay topology that allows the production of high energetic muons and a cross section which is about six orders of magnitude larger than the corresponding cross section of the signal. In order to provide sufficient statistics for this channel, a data sample corresponding to an integrated luminosity of 2077 nb^{-1} was generated. Six events have passed the cuts. After application of a cut on the invariant mass of the muons to be above 70 GeV, no event survives. The upper limit on background from the process $pp \to b\bar{b} \to \mu^+\mu^- + X$ is 0.27% of the signal at the 95% confidence level.

Cut	events remaining
exactly 2 μ's reconstructed	40.9%
$p^T_\mu \geq \frac{M_Z}{M_W} \cdot 25$ GeV	28.3%
$\lvert\eta^\mu\rvert \leq 2.3$	27.1%
$\lvert\vec{u}\rvert \leq 20$ GeV & # jets ≤ 1, $p^T_{jet} \leq 30$ GeV	16.6%

Table 4: Consecutive selection cuts for generated events of the process $Z \to \mu^+\mu^-$. In the right column the remaining fraction of events after each cut is listed. $\vec{u}$ represents the hadronic recoil.

Cut	events remaining
exactly one μ reconstructed	58.2%
$p_\mu^T \geq 25$ GeV	40.8%
$E_{miss}^T \geq 25$ GeV	35.9%
$\lvert\eta^\mu\rvert \leq 2.3$	34.57%
$\lvert\vec{u}\rvert \leq 20$ GeV & # jets ≤ 1, $p_{jet}^T \leq 30$ GeV	23.68%

Table 5: Consecutive selection cuts for generated events of the process $W \to \mu\nu$. In the right column, the remaining fraction of events after each cut is listed. $\vec{u}$ represents the hadronic recoil.

Note that no isolation criteria on the muons have been used so far; these will significantly reduce the background. A corresponding study, however, needs very large samples of fully simulated events, which are not available at present. Similar considerations hold for background processes like $c\bar{c} \to \mu^+\mu^- + X$ and $s\bar{s} \to \mu^+\mu^- + X$. The cross section is larger, but the muon spectrum in jets containing c or s quarks is softer than for b quarks. With small statistics of about 500 nb^{-1} for each of the processes, no event passes the preselection cuts. Therefore, an upper limit for the contribution of each of the processes to the signal, before application of any isolation criterion, is about 1.2%.

5.1.3 W Boson Event Selection

The HLT threshold for single muon events is 19 GeV and the corresponding cuts are chosen with the same reasoning as for the Z boson events. To accept an event, the lower limit on momentum of an isolated muon and its pseudo-rapidity is set to 25 GeV and $|\eta| \leq 2.3$. In addition, the missing transverse energy, E_{miss}^T, measured in an event has to exceed 25 GeV in order to improve the probability that a neutrino is contained in the final state. For the hadronic recoil, which is determined from the missing transverse energy measured in the calorimeter, $|\vec{u}| \leq 20$ GeV is required. Events with at least one extra jet with $p_{jet}^T \geq 30$ GeV or with more than one jet are also discarded. The last two cuts reject W bosons produced with high transverse momentum. A summary of the applied selection cuts and the fraction of remaining W events after each cut is presented in Table 5.

The transverse mass is reconstructed from the measured lepton p^T in the tracking and muon detectors as well as from the calorimetric measurement of the missing transverse energy, $E_{\mathrm{mis,calo}}^T$. The total missing energy in the event is then obtained by $E_{\mathrm{miss}}^T = E_{\mathrm{miss,calo}}^T - p_\mu^T$, and corresponds to the transverse momentum of the undetected neutrino. $E_{\mathrm{miss,calo}}^T$ corresponds to the hadronic recoil $\vec{u}$ in the event, which is equal to the transverse momentum of the W boson. The transverse mass then becomes

$$m^T = \sqrt{2p_\mu^T(E_{\mathrm{miss,calo}}^T - p_\mu^T)(1 - \cos(p_\mu^T, E_{\mathrm{miss}}^T))}. \tag{15}$$

The cut on the hadronic recoil, as listed above, ensures that the transverse mass is dominated by the measurement of the lepton p^T. It is, however, evident, that the transverse mass is sensitive to fluctuations in the calorimetric missing transverse energy, caused either by resolution, detector inhomogeneities or pile-up.

With the cuts described above, most of the background is suppressed. However, Z bosons decaying into two muons with one of them not being detected constitute an irreducible background. The non-identification of a muon as missing energy can have two causes: the muon was not reconstructed, or it did not passed through the region of the CMS detector instrumented with muon chambers. Events of the first case might be reduced by applying cuts at the level of muon hits. One might be tempted to reject events of the second case by requiring that the missing energy points into the acceptance region for muons. This can in principle be determined using a W mass constraint. In addition, the resolution of the longitudinal component of the missing energy is not sufficient. In Fig. 21, the contribution of Z boson events to the W sample is shown.

The distribution of the background is flattish, but situated in the region of the Jacobian edge. Current results from the DØ collaboration as well show such a background at a comparable level [21].

Another source of backgrounds stems from the process $pp \to b\bar{b} \to \mu + X$, which provides events similar to a typical W signature and might therefore fake signal events. As its investigation needs a large statistics of fully simulated events and its contribution is expected to be small, it is not studied here.

The process $W \to \tau\nu$ with $\tau \to \mu\nu\nu$ is estimated to amount to 1.3% [22]. This background is suppressed by the cut on the muon momentum, as the neutrinos carry away a large fraction of the momentum. At DØ, this contribution is very small and occurs mainly up to 75 GeV in the transverse mass spectrum [21], well below the Jacobian edge.

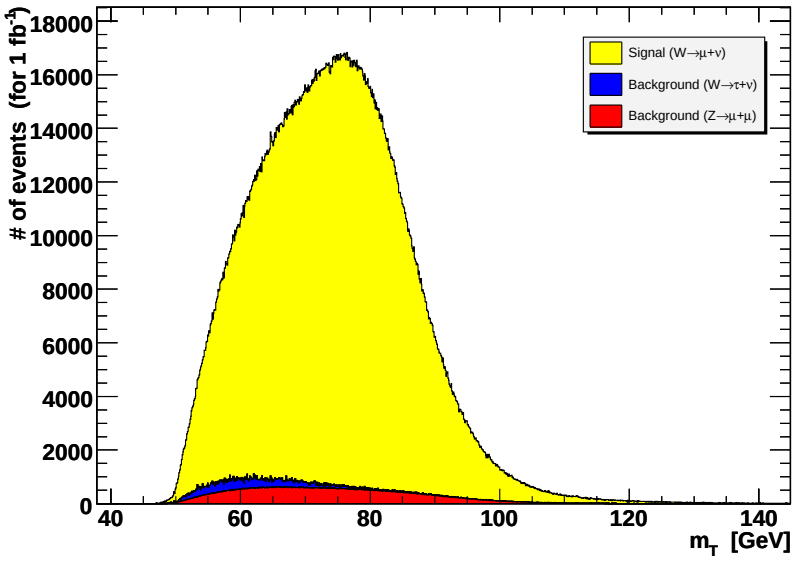

Figure 21: FAMOS simulation of the W signal with the expected contribution of background processes. The yellow area (light-coloured) represents the W signal. In blue (dark) the contribution from the process $W \to \tau\nu$ is shown which does not affect the region of the Jacobian edge. The red area (grey) shows the contribution of background processes $pp \to Z^0/\gamma^* \to \mu^+\mu^-$ to the signal which is placed in the region of the Jacobian edge. All distributions are scaled to an integrated luminosity of 1 fb^{-1}.

5.2 Measurement of the W Boson Mass

The event sample obtained from the fast detector simulation is the basis for the studies presented below. This is justified as these are meant to demonstrate the principle and allow for studies of various systematic effects. Thus, areas of importance will be identified where reliable simulation and validation of the underlying physics and of the detector performance are needed. The selection cuts listed above define a working point of the analysis around which systemic uncertainties are evaluated.

5.2.1 Weight factors

In order to obtain a prediction of the distribution of the transverse W mass from measured Z events, it is not sufficient to perform the kinematical manipulations described above (see section 2.2), because there are additional differences between the Z and W bosons, which have to be taken into account:

1. the η and p^T distributions of the produced W and Z bosons are slightly different;
2. the Z sample contains an irreducible contribution from Drell-Yan events produced via virtual photons;
3. in a Z event, both leptons can radiate, in contrast to the neutrino from W decay;
4. the Z sample only contains events with both leptons inside the acceptance of the muon detector, while only one muon inside the acceptance is required for W events.

In Fig. 22, the ratio of the reconstructed distributions in transverse mass for W and transformed Z-bosons is shown. The transformation only includes the adjustment of the Z boson mass and width to the W mass and width, as described above, without any further re-weighting of the Z events. Sequentially applying cuts on p_μ^T, η, the recoil $|\vec{u}|$, p_{rec}^T, and finally introducing the full detector as simulated with FAMOS, leads to the deviations between the distributions illustrated in the figure. The cuts have a large effect at low values of the transverse mass distribution, which therefore cannot be reliably used to determine the W mass and width. At very high values exceeding 90 GeV, the statistics is low, and hence the sensitivity to the W mass is also small. In the critical region around the Jacobian edge, the differences remain within $\pm 20\%$.

For further illustration, Fig. 23 shows the transverse mass distribution of W and morphed Z events at generator level and after all cuts with full detector simulation using FAMOS.

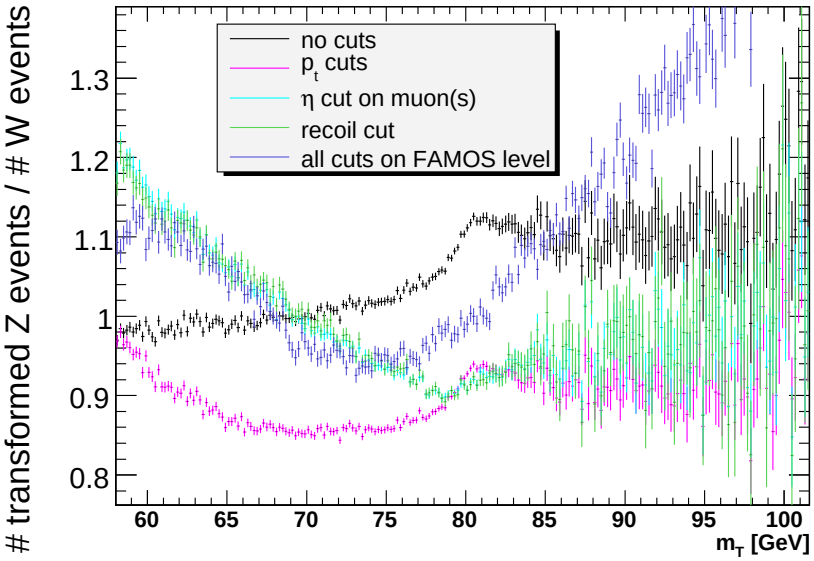

Figure 22: Ratios of the distributions in transverse mass of W bosons and transformed Z bosons are shown in this figure for different cuts applied sequentially. The ratios are calculated by dividing the distributions of the morphed Z boson transverse mass by the distributions in transverse mass of the W boson.

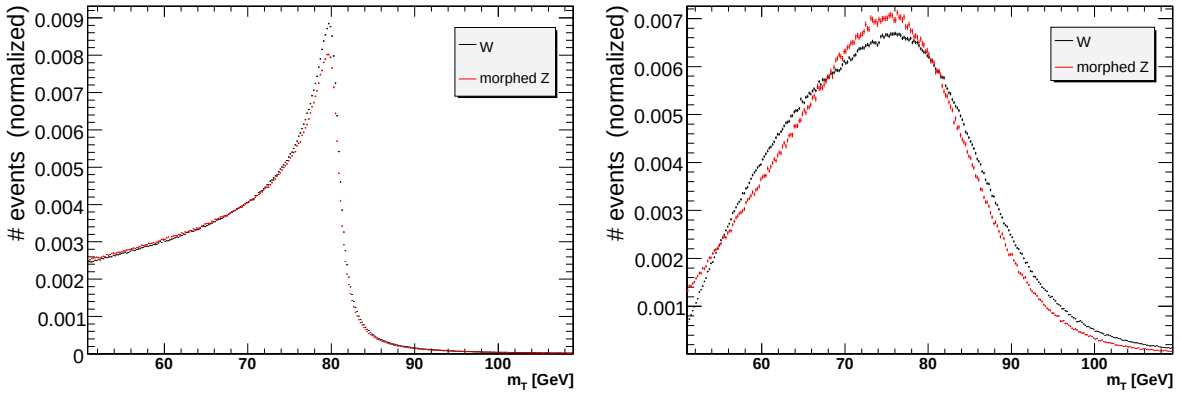

Figure 23: *Left*: In black, the transverse mass distribution of generated W events without cuts is shown. In red the corresponding distribution of Z boson events, morphed to the mass of the generated W bosons, is shown.
Right: The same distributions after FAMOS simulation and application of all selection cuts.

5.2.2 Mass fit

The ratio of the transverse mass distributions given in Fig. 22 is taken as the basis to determine re-weighting factors $w(m^T)$ applied to morphed Z events. These weights take into account all effects beyond the analytical transformations to account for the difference in mass and width of W and Z bosons. Smoothing is done by approximation by a fifth order polynomial. After applying the weights, the transverse mass distributions of W and morphed Z events agree at the generated W boson mass. To demonstrate the application of the method and to determine the statistical precision of the W mass measurement, Z boson events are morphed to different masses M_Z^{morph}, chosen in steps of 1 MeV. This is followed by the application of the weights $w(m^T)$. The resulting transverse mass distributions are compared with the generated m^T distribution of the W bosons. The comparison is based on a χ^2 criterion which characterises the compatibility of the two histograms,

$$\chi^2 = \sum_i \frac{\left(N_i^W - N_i^Z\right)^2}{\sigma_{i,W}^2 + \sigma_{i,Z}^2}\,, \tag{16}$$

where i indicates the bin number. N_i is the number of entries in bin i and σ_i represents the uncertainty of N_i.

The χ^2 values for different transverse mass values are expected to lie on a parabola, from which the best-fit value and the statistical precision of the method are determined. Figure 24 shows the difference in χ^2 with respect to the minimum as a function of the difference between M_Z^{morph} and the generated W mass for the full available Monte Carlo statistics. The number of events and the errors in each histogram bin are scaled to correspond to an integrated luminosity of 1fb^{-1}. The minimum lies at a value of 3 MeV showing the self-consistency of the method, expected resolution on the W mass determined from the parabola shown in the figure is ± 39.0 MeV. When not scaling down to an integrated luminosity of 1 fb^{-1}, the χ^2 value at the minimum is about 1 per degree of freedom.

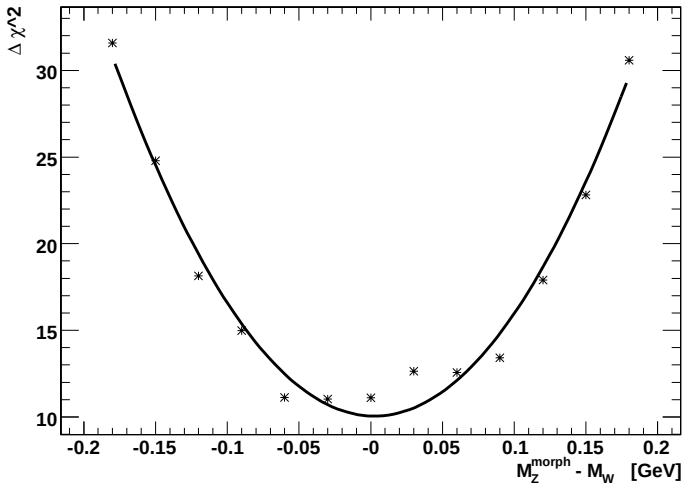

Figure 24: $\Delta\chi^2$ distribution for the comparison of the transverse mass distributions from morphed Z and W events as a function of the difference between M_Z^{morph} and M_W for an integrated luminosity of 1 fb^{-1}. The expected resolution on M_W determined from the parabola is ± 39 MeV.

5.2.3 Systematic Effects

The working point, defined in the previous subsection, forces the distributions in transverse mass to agree perfectly by the application of appropriate weights. Effects on the W mass of cuts, detector alignment, the muon momentum scale, parton density functions etc. are evaluated by variation of the corresponding observables around this working point in the following paragraphs.

Muon momentum scale and resolution The measured transverse mass depends directly on the muon momentum scale, which is determined by the precision of the mappig of the magnetic field. In the proposed mehtod, cancellations between the Z and W samples are expected to occur. Changing the transverse momenta of the reconstructed muons by a huge amount of ± 1 % shifts the minimum of the χ^2 parabola by only 140 MeV, as is shown

in Fig. 25, while the transverse mass distribution of the W itself shifts by 800 MeV. For a precision of 0.1%, the systematic error is only 14 MeV.

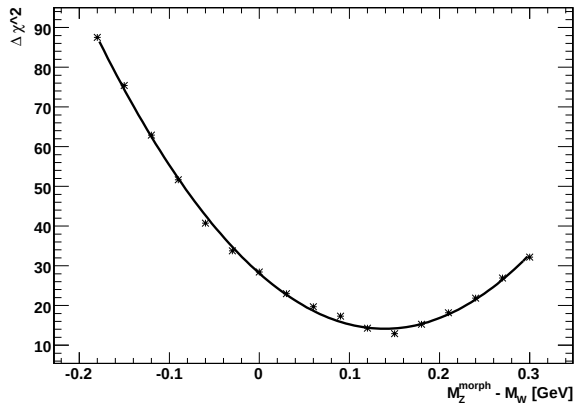

Figure 25: χ^2 comparison for calorimeter muon scale decreased by 1%. The minimum of the parabolic fit is at 140 MeV.

As a test for the sensitivity to the correct description of the muon momentum resolution, an additional Gaussian smearing of 10 % of the RMS resolution ($\mathrm{RMS}_{\mu,1/p_T} = 7.4 \cdot 10^{-4}$/GeV) of the inverse of the reconstructed momentum was applied to the inverse of the reconstructed momenta, leading to an effect on the W mass of 30 MeV. Rather precise understanding and modelling of the detector resolution will be mandatory for a precision measurement of the W mass. This is probably not possible with the initial detector alignment achievable with the first fb^{-1} of integrated luminosity.

Angular offsets and resolution The precision of the acceptance definition also enters the W mass measurement. Such dependencies are studied by systematically shifting the reconstructed values of θ and η of the muons. The dependence on the angular resolution was studied by applying an additional Gaussian smearing of 10 % of the resolution to the reconstructed value of θ. As a natural scale, the RMS resolution in θ, σ_θ, was chosen. A systematic shift in the reconstructed θ value by $\sigma_\theta = 3 \cdot 10^{-4}$, which may be caused e.g. by displacements of the luminous region of the colliding beams w.r.t. the centre of the detector, lead to a relatively large effect of 19 MeV. The modelling of the θ resolution is rather uncritical, if it can be described with a precision of 10%. If the boundaries in acceptance have an uncertainty corresponding the the resolution in η, which is $\sigma_\eta = 6 \cdot 10^{-3}$, an effect of about 20 MeV on the W mass is observed.

Nonlinearities in momentum scale While a number of experimental and systematic effects cancel in the proposed method, nonlinearities of the momentum or energy scale will enter unsuppressed. The lepton momentum scale at $\frac{M_Z}{2}$ can be fixed quite precisely using the Z sample, and studies of sub-samples with special decay topologies will allow to check the momentum scale at lower momenta. With a simple parameterisation of the non-linearities in muon momentum scale, see Equation 6, the expected effect on the W mass is about 10 MeV for a value of the non-linearity parameter of $\epsilon = 2 \cdot 10^{-5}$/GeV. Since transverse mass in the muon channel depends mainly on the measurement of track curvatures in a magnetic field, which are proportional to $1/p^T$, non-linearities in the momentum scale are expected to be negligible.

Calorimeter MET scale The missing transverse energy in an event is composed of the missing transverse energy measured in the calorimeters $E^T_{\mathrm{miss,calo}}$, and the measured momenta of the reconstructed muon(s). In Z events, $E^T_{\mathrm{miss,calo}}$ is identical to the reconstructed transverse momentum of the Z boson, which can be determined rather precisely from the two muons. In W$\rightarrow \mu\nu$ events, $E^T_{\mathrm{miss,calo}}$ corresponds to the transverse momentum of the W. $E^T_{\mathrm{miss,calo}}$ can thus be calibrated using the reconstructed transverse momenta of the muons in $Z \rightarrow \mu^+\mu^-$ events. Figure 26 shows that this calibration works well to provide, on average, a good measure of the W boson p^T. The fitted slope of 0.984 deviates from from the ideal case of a slope of 1 by less than about 2%, which is taken as the systematic scale uncertainty on $E^T_{\mathrm{miss,calo}}$.

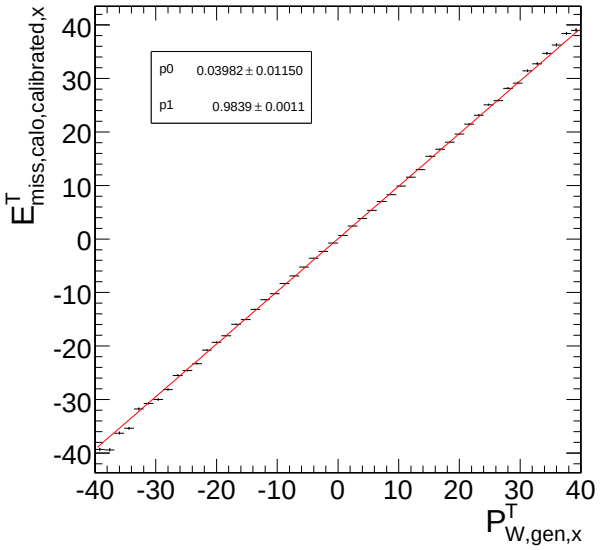

Figure 26: X-Component of the calibrated missing transverse energy in the calorimeter as a function of the transverse W boson momentum at generator level. The slope of a fitted straight line is 0.984.

In order to investigate the sensitivity of the morphing method to such an uncertainty in the calorimeter MET scale, $E^T_{\text{miss,calo}}$ was changed by $\pm 2\,\%$. The χ^2 minimum shifts to -38 MeV and $+38$ MeV, respectively. Although the scale uncertainty is large compared to the level of precision to be reached on the W mass, the effect on M_W is rather small due the cut on the hadronic recoil, which ensures that the transverse mass is mostly dominated by the measured muon p^T, see Equation 15.

Since the resolution on the missing energy from the calorimeter is very poor, significant effects are expected from the modelling of the resolution in $E^T_{\text{miss,calo}}$. The resolution of $E^T_{\text{miss,calo}}$ can be measured from Z events by comparison with the reconstructed p^T of the Z boson, determined from the momentum sum of the two muons. The relevant distributions from the simulation with FAMOS are shown in Fig. 27. The resulting width is about 6% smaller than the width of the distribution of the differences between $E^T_{\text{miss,calo}}$ and P^T_W. Such differences are expected due to radiative W decays, in which the transverse energy of photons radiated from a muon is also measured as calorimetric transverse energy. Although most of this difference will probably be understood, conservatively, a systematic error of 5% on the modelling of the resolution in missing energy in the calorimeters is assumed as the systematic error for the initial detector. Increasing the difference between the true and the reconstructed missing transverse energy in the calorimeters by 5%, separately for the x and y components, results in an effect on M_W of 30 MeV.

The poor resolution in $E^T_{\text{miss,calo}}$ is the main origin for the smearing-out of the Jacobian edge in the transverse mass distribution, and explains the large systematic errors arising from the modelling of the measurement of the missing transverse energy in the calorimeters. Crucial to the successful application of the suggested method is a very good description of $E^T_{\text{miss,calo}}$ in the Monte Carlo, including pile-up effects, which depend on the instantaneous luminosity and are therefore time-dependent. Again, the sample of Z events is extremely important for the verification of the simulation.

W width Effects of the uncertainty in the width, Γ_W, were easily included by changing the W width in transformation procedure by its present experimental error [6]. The influence is rather weak, ± 10 MeV on the W mass.

Alignment of the early detector The alignment of the early detector after the analysis of an integrated luminosity of 1 fb^{-1} is significantly worse than the perfectly aligned detector, leading to a resolution in p^T which is about two times worse (see Figure 9.12 in [9]). The effect of the larger uncertainties with the early detector were simulated by applying an additional smearing in $1/p^T$ to the muon momenta of all Z and W events in the available Monte Carlo sample. The resulting total resolution in W mass with the early detector is thus estimated to be 40.8 MeV, instead of 39.0 MeV with the perfectly aligned detector. The extra uncertainty on the W mass arising from alignment

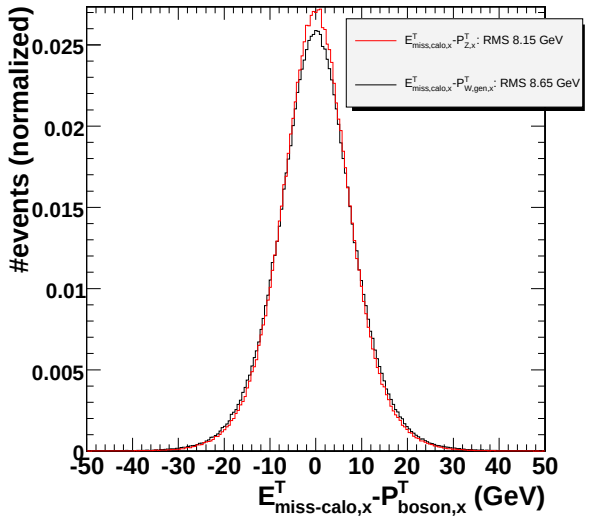

Figure 27: Distributions of $E^T_{\mathrm{miss,calo,x}} - P^T_{\mathrm{Z,x}}$ (from the reconstructed transverse momentum of Z bosons, red/grey line), and $E^T_{\mathrm{miss,calo,x}} - P^T_{\mathrm{W},gen,x}$ (from the transverse momentum at generator level for W bosons, black line), after all cuts. The widths of the two distributions differ by 6.1%.

uncertainties is thus estimated to be only 12 MeV.

Background modelling To give an estimate on effects concerning the understanding of the background in the W events, as an exemplary study concerning misidentified Z events as the most important background has been perfomed. For this, the effect of an over-/underestimatation of the background at the 10% level is applied whereas the weights remain unchanged. For the best fit value of the W mass, a shift of 4 MeV is observed.

Parton density functions The effect of a variation of the parton density function has been studied in detail for the scaled p^T-lepton method in the electron case, and the effects are assumed to be of a similar size for the morphing method.

Theoretical errors In the study presented, the main emphasis was given to purely experimental aspects of the method. In addition, there are potentially large theoretical errors, arising from differences in the p^T spectra of W and Z bosons and from QED and electroweak effects in the Z or W boson decay. These are important for the correct description of the acceptance for the second muon in a Z event, which is turned into a neutrino in order to simulate a W event. Further studies involving next-to-leading order QCD calculations and higher-oder electroweak corrections will need to be performed for a full evaluation of all errors.

5.2.4 Summary of systematic effects

The systematic effects studied in the previous sub-sections are summarised in Table 6. The last column in the table specifies the level to which each source of uncertainty needs to be restricted if a systematic uncertainty of ± 10 MeV is to be achieved on the W boson mass.

5.3 Using the p^T-lepton method with muons

Using only the muon p^T as the experimental observable for the determination of the W mass, *i.e.* applying the scaled-observable method, as described above, has also been studied on the available sample of $W \to \mu\nu$ and $Z \to \mu^+\mu^-$ events. Again, the weights have been computed using the full statistics at the nominal W mass, and were then applied to the different test values for the W boson mass. A better resolution of ± 30 MeV is observed (see Figure 28), which is better than the one obtained for the morphing method, because, experimentally, the lepton p^T has a higher precision than the transverse mass. Systematics have not been studied in detail, but is expected to be comparable to the electron case. The resolution obtained from the muon sample is better than in the electron

source of effect and size variation	shift of reconstructed W mass	10 MeV effect on M_W
background by 10%	4 MeV	25%
muon momentum scale by 0.1%	14 MeV	0.07%
muon $1/p^T$ resolution smeared by 10%	30 MeV	3%
Nonlinearities in momentum scale	expected to be negligible	-
muon θ resolution smeared by 10%	3 MeV	30%
systematic shift in muon η $\pm$ resolution	19 MeV	0.5 σ_η
reduction/expansion of η acceptance $\pm$ resolution	17 MeV	0.6 σ_η
calorimeter MET scale by 2%	38 MeV	0.5%
calorimeter MET resolution by 5%	30 MeV	1.7%
W width $\pm 1\sigma_{\Gamma_W}$	10 MeV	$1\sigma_{\Gamma_W}$
detector alignment for 1 fb^{-1}	12 MeV	
PDF errors	similar to electrons, 20 MeV	
other theory errors	not yet evaluated for this experimental study	

Table 6: Summary of systematic effects. The last column gives the precision needed in order to restrict the systematic error on the W mass to $\pm$10 MeV.

case, because the number of $Z \to \mu^+\mu^-$ events surviving the cuts is larger than the number of electrons after cuts (see Tables 4.1, 4 and 5).

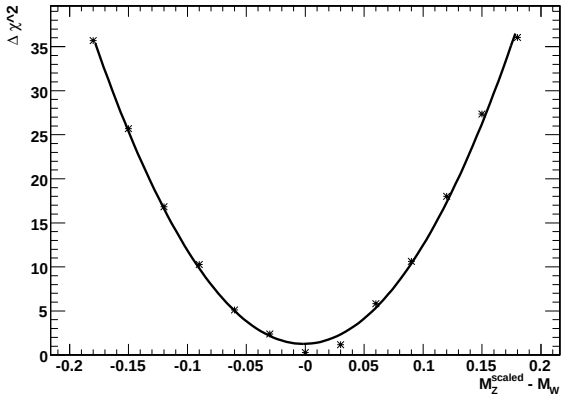

Figure 28: $\Delta\chi^2$ distribution for the lepton method used on the muons for 1 fb^{-1}. The best fit value lies 1 MeV below the generator W mass. The resolution is 30 MeV.

6 Comparison of the two Analyses

In the previous sections studies of systematic effects on the measurement have been described, and the sensitivities of M_W to detector systematics have been summarised in Table 2 for the scaled E^T-lepton method applied to the electron channel and in Table 6 for the morphing method applied to the muon channel.

The expected size of various detector effects for the early detector, after the analysis of an initial integrated luminosity of 1 fb^{-1}and for a better detector understanding expected after employing an integrated luminosity of 10 fb^{-1}, is shown in Table 7, together with the resulting uncertainties on M_W.

The measurements of the W mass by means of $W \to e\nu$ and $W \to \mu\nu$ decays are largely independent. The analysis based on the electron E^T measurement is limited by the uncertainty related to the $p^T(W)$ prediction, to which the m^T distribution is instead only slightly sensitive. On the other side, the uncertainties on the calorimeter MET scale and resolution affect mostly the analysis of the m^T spectrum because in this case the missing transverse energy measurement enters directly in the determination of the observable m^T from which M_W is extracted, but only indirectly through the events selection in the lepton E^T study. Differences in the impact of the lepton scale and resolution between the two methods come mainly from the different shape of the re-weighting functions used in the two procedures (see Fig. 9 for the scaled E^T analysis using electrons, and Fig. 22 for the transverse mass in the muon channel). From Table 7, it becomes clear that the scaled p^T-lepton method suffers less from experimental systematic errors than the morphing method, which is dominated by uncertainties arising from the measurement of the missing transverse energy in the calorimeters. If systematic errors arising from the theoretical prediction of the transverse momenta of the Z and W bosons can be brought to a level of $\sim$10 MeV, the scaled p^T-lepton method is clearly the first choice. The full error analysis using the scaled p^T-lepton method for the muons has not yet been performed, but can be deduced from the study performed with the electrons. The higher acceptance for muons leads to a better statistical precision of 30 MeV for 1fb^{-1}, and the errors arising from the muon momentum scale are smaller than the errors due to the electron energy scale. Errors due to the recoil modelling are identical and fully correlated with the electrons. The total instrumental error from the muon channel can thus be estimated to be about 25 MeV for the initial measurement with an integrated luminosity of 1fb^{-1}. The error component in common with the electrons amounts to about 20 MeV. Clearly, all theoretical errors are of the same size and fully correlated between the electron and muon channels.

The morphing method has the advantage of providing templates for observables in W events from measured observables in Z events. In particular, the measurement of the transverse momentum of Z bosons and the cross checks on the modelling of the missing energy are of vital importance to quantify systematic uncertainties.

The combination of the electron and muon channels brings the statistical error to a final precision of better than 10 MeV, and a systematic resolution of instrumental origin below 20 MeV.

Source of uncertainty	electron channel				muon channel			
	with 1 fb^{-1}		with 10 fb^{-1}		with 1 fb^{-1}		with 10 fb^{-1}	
	assumed uncertainty	ΔM_W	assumed uncertainty	ΔM_W	assumed uncertainty	ΔM_W	assumed uncertainty	ΔM_W
statistics		**40 MeV**		**15 MeV**		**40 MeV**		**15 MeV**
background	10%	10 MeV	2%	2 MeV	10%	4 MeV	2%	negligible
lepton								
energy/momentum scale	0.25%	10 MeV	0.05%	2 MeV	0.1%	14 MeV	$<$0.1%	$<$10 MeV
energy/momentum linearity	6×10^{-5} GeV^{-1}	30 MeV	$<2\times10^{-5}$ GeV^{-1}	$<$10 MeV	expected to be negligible	negligible	expected to be negligible	negligible
energy/momentum resolution	8%	5 MeV	3%	2 MeV	10%	30 MeV	$<$3%	$<$10 MeV
acceptance	resolution in η	2 MeV	resolution in η	2 MeV	resolution in η	19 MeV	$< \sigma_\eta$	$<$10 MeV
detector alignment						12 MeV		negligible
MET scale	2%	15 MeV	$<$1.5%	$<$10 MeV	2%	38 MeV	$\leq$1%	$<$ 20 MeV
MET resolution	5%	9 MeV	$<$2.5%	$<$ 5 MeV	5%	30 MeV	$<$3%	$<$18 MeV
recoil system	2%	15 MeV	$<$1.5%	$<$10 MeV				
total instrumental		**40 MeV**		**$<$20 MeV**		**64 MeV**		**$<$30 MeV**
PDF uncertainties		20 MeV		$<$10 MeV		$\sim$20 MeV		$<$10 MeV
Γ_W		15 MeV		$<$15		10 MeV		$<$ 10 MeV
$p^T(W)$		30 MeV		30 MeV (or NNLO)				
other theory errors	not yet evaluated for this experimental study				not yet evaluated for this experimental study			

Table 7: Expected systematic errors on M_W for the scaled E^T-lepton method with electrons and for the morphing method with muons. The first column lists the systematic effect considered. Columns 2-5 (electron channel) show the assumed detector uncertainty for an initial integrated luminosity of 1 fb^{-1}, the resulting uncertainty on M_W and the extrapolation to an integrated luminosity of 10 fb^{-1} when the detector understanding is assumed to have significantly improved. The last four columns show the expected uncertainties with 1 fb^{-1}and the extrapolation to 10 fb^{-1} for the M_W measurement in the muon channel.

7 Summary and conclusions

The precise measurement of the mass of the W boson constitutes an important consistency check of the Standard Model and is sensitive to supersymmetric corrections. Together with the top quark mass, the W mass discriminates between the Standard Model and supersymmetric extensions. In this note, methods have been presented which employ the large number of Z bosons produced at the LHC to significantly reduce theoretical and experimental uncertainties on the W mass measurement.

Two complementary approaches have been developed and applied to the analysis of $W \to e\nu$ and $W \to \mu\nu$ decays. The former analysis, based on the measurement of the transverse electron energy, can be fully exploited with the first 1 fb^{-1} of collected data, as procedure to keep the systematic uncertainties to a level comparable to the statistical precision (around 40 MeV) have been envisaged. A final precision on the W mass for 10 fb^{-1} of integrated luminosity of about 15 MeV (stat.) and below 20 MeV (syst.) is expected. Some ambiguity still remains on the uncertainty related to the theoretical calculation of the electron E^T spectrum. Yet, the impact of these effects is expected to be largely reduced by the analysis strategy adopted.

The analysis of $W \to \mu\nu$ has considered the transverse mass distribution. While the required precision in the measurement of the muon momentum might be difficult with the first data sets, a final precision comparable to the one achievable with the electrons is expected. This observable, moreover, is less affected by theoretical uncertainties.

The two methods rely on different parts of the detector and exploits different observables. Thus a combination with little common uncertainties (mainly related to the PDF) is anticipated. This would bring the final precision of the CMS experiment on the W mass at the 20 MeV level or better.

Acknowledgements

We gratefully acknowledge D. Bourilkov, for useful suggestions on the evaluation of the PDF uncertainties, A Banfi and C. Oleari, for discussions about the uncertainty related to the p-QCD calculation of the scaled observables ratios. All the members of the Standard Model group in CMS, and in particular J. Mnich, are acknowledged for criticism, suggestions and discussions that helped improve this work.

A special thanks to Christophe Saout, whose expertise in computing was of great help.

References

[1] CERN-TH/2000-102 S. Haywood, P. R. Hobson, W. Hollik, Z. Kunszt et al. *Electroweak physics* (2000)

[2] CMS CR 2003/039 C. K. Mackay, *Electroweak Physics and the Top Quark Mass at the Large Hadron Collider* (2003)

[3] CERN/LHCC 94-14 and 99-15 CMS Collaboration, *CMS Detector and Physics Performance Technical Design Report* (1994)

[4] W. T. Giele, S. Keller, Phys.Rev.D57:4433-4440 (1998)

[5] A. Schmidt, *Development of Analysis Software and Determination of W Boson Parameters by Comparison with Z Bosons at the LHC*,
Diplomathesis, IEKP-KA/2004-2, (2004)
www-ekp.physik.uni-karlsruhe.de/pub/web/thesis/schmidt_dipl.pdf

[6] S. Eidelman *et. al.*, *Particle Physics Booklet*. Particle Data Group, July 2004.

[7] T. Sjöstrand, L. Lönnblad, S. Mrenna, *PYTHIA 6.2 Physics and Manual*, arXiv:hep-ph/0108264

[8] V.Karimäki, *CMKIN, CMS Physics Generator Interface*,
`http://cmsdoc.cern.ch/cmsoo/projects/CMKIN/`

[9] CERN/LHCC 2006-001 CMS Collaboration, *CMS Physics Technical Design Report, Volume I: Detector Performance and Software* (2006)

[10] T. Affolder et al., *Measurement of the W Boson Mass with the Collider Detector at Fermilab*, arXiv:hep-ex/0007044 v3 (2001)

[11] CMS NOTE 2006/039 P.Meridiani, R.Paramatti, *Use of $Z \to e^+e^-$ events for ECAL calibration* (2006)

[12] J. Pumplin et al., JHEP 0310:046,2003.

[13] A.D. Martin, R.G. Roberts, W.J. Stirling, R.S. Thorne, Eur.Phys.J. C28 (2003) 455-473;

[14] A.D. Martin, R.G. Roberts, W.J. Stirling, R.S. Thorne, arXiv:hep-ph/0307262;

[15] A.D. Martin, R.G. Roberts, W.J. Stirling, R.S. Thorne, Phys.Lett. B604 (2004) 61-68.

[16] LHAPDF library v. 4.2, S. Alekhin, M. Botje, W. Giele, J. Pumplin, F. Olness, G. Salam and A. Vogt, *Physics at TeV Colliders II Workshop* , Les Houches, France, May 2001.

[17] D. Stump et al., Phys.Rev.D65:014012, 2002, J. Pumplin et al, Phys.Rev.D65:014013,2002

[18] P.M.Nadolsky and Z. Sullivan, *PDF uncertainties in WH production at Tevatron*, eConf C010630:P510,2001 and arXiv:hep-ph/0110378 (2001)

[19] W.T. Giele, E.W.N. Glover, David A. Kosower; arXiv:hep-ph/9302225., Nucl.Phys.B403:633-670,1993.

[20] CERN/LHCC 2002-026 CMS Collaboration, *Data Acquisition & High-Level Trigger Technical Design Report Volume 2*, 15 December 2002

[21] S. Leone, INFN Pisa: Review of W and Z physics at the Tevatron
HEP EPS Lisbon, July 21-27 2005

[22] *Proceedings of the Workshop on Standard Model Physics (and more) at the LHC (CERN 2000-004)*, 2000